Building and Environment 209 (2022) 108656

Contents lists available at ScienceDirect

Building and Environment

journal homepage: www.elsevier.com/locate/buildenv

A novel LCSA-Machine learning based optimization model for sustainable building design-A case study of energy storage systems

Hashem Amini Toosi *, Monica Lavagna, Fabrizio Leonforte, Claudio Del Pero, Niccolò Aste

Architecture, Built Environment and Construction Engineering Department, Politecnico di Milano, Via Ponzio 31, 20133, Milano, Italy

ARTICLE INFO

Keywords:
Life cycle sustainability assessment
Building energy retrofitting
Energy storage
Optimization
Machine learning

ABSTRACT

Life Cycle Sustainability Assessment (LCSA) in the built environment has increasingly drawn researchers' attention in the preceding years; however, the lack of an integrated LCSA based model is still a barrier for its effective implementation into the building design process.

This paper proposes a new comprehensive LCSA model to be integrated into the design process of new buildings and energy refurbishment scenarios of existing ones. The proposed model consists of sets of mathematic equations to describe LCSA pillars of buildings, including Life Cycle Assessment (LCA), Life Cycle Costing (LCC), and Social Life Cycle Assessment (SLCA) as the intermediate indices. A final LCSA index is then provided to describe a design scenario's performance from an LCSA perspective using the authors' new formulation and weighting method. The model is also integrated into the optimization process and enhanced with Machine Learning (ML) methods to accelerate the design-assessment process while preserving its accuracy. Finally, given the transition towards buildings' electrification by Renewable Energy Sources (RESs), as a supportive technology, the size-optimization of a residential building's short-term thermal and electrical Energy Storage Systems (ESSs) is chosen to demonstrate the model's capabilities. For this purpose, the building case study is parametrically modeled in Grasshopper, Energy plus, and Matlab for energy analysis, data processing, and machine learning.

1. Introduction

The built environment is rapidly expanding in response to the growing needs of housing and development [1]. In this context, the significant shares of building construction and operations in the global final energy consumption and energy-related CO_2 emission are estimated at 36 and 39%, respectively [2]. At the European Union (EU) level, the building sector is accounted for about 40 and 32% of the energy consumption and carbon emission, correspondingly [3]. The noticeable contribution of the built environment expansion to the environmental impacts [4,5], economy, and societies [6], known as three pillars of sustainable development [7], has progressively drawn researchers' attention inside academies, industries, and policy programs. The perception of considerable impacts of the construction and building sector on sustainability targets has led to establishing standards and guidelines to reduce the building sector's environmental impacts. Given the sustainability concerns, the environmental aspects and economic and social performance have been pursued by emerging studies to provide harmony and balance among the three sustainability pillars [8].

Energy efficiency directives such as Directive 2002/91/EC, Directive 2006/32/EC, and Directive 2010/31/EC [9,10,11] have been designed, widely accepted, and implemented in the building sector to control and mitigate the energy consumption of the buildings within their operational phase. However, recent studies revealed that the successful implementation of the energy efficiency codes decreases the buildings' energy consumption in the operational phase, but it might cause an environmental load-shift towards other life cycle phases [12,13]. As a piece of evidence, the buildings' embodied impact is estimated to become equivalent to their operational impact by 2050 [14]. This upcoming phenomenon highlights the importance of a whole life cycle thinking approach to the building sector.

A Life Cycle Sustainable Assessment (LCSA) approach to building design aims to evaluate buildings' environmental (LCA), economic (LCC), and social (SLCA) performance throughout the whole life cycle phases of the buildings [15,16]. LCSA is known and is applied as a comprehensive and promising method to evaluate the sustainability performance of the built environment [17].

The building sustainability assessment methodologies could be categorized into the frameworks developed by international standards

* Corresponding author.
E-mail address: hashem.amini@polimi.it (H. Amini Toosi).

https://doi.org/10.1016/j.buildenv.2021.108656
Received 18 August 2021; Received in revised form 1 November 2021; Accepted 3 December 2021
Available online 8 December 2021

Nomenclature

AI	Artificial Intelligence
ANN	Artificial Neural Network
AP	Acidification Potential
BAU	Business As Usual
COP	Coefficient of Performance of Heat Pump
DHW	Domestic Hot Water
$DoD_{battery}$	Battery's Depth of Discharge
DR	Discount Rate
EP	Eutrophication Potential
ERMs	Energy Retrofit Measures
ESSs	Energy Storage Systems
GBRSs	Green Building Rating Systems
GPR	Gaussian Process Regression
GWP	Global Warming Potential
HP	Heat Pump
Li-ion	Lithium-ion
ML	Machine Learning
LCA	Life Cycle Assessment
LCC	Life Cycle Costing
LCIA	Life Cycle Impact Assessment
LCSA	Life Cycle Sustainability Assessment
NPV	Net Present Value
ODP	Ozone Depletion Potential
PIR	Price Inflation Rate
POCP	Photochemical Ozone Creation Potential
RESs	Renewable Energy Sources
RMSE	Root Mean Square Error
RU-m	Resource Use-minerals & metal
RU-f	Resource Use-fossils
SD	Standard Deviation
SLCA	Social Life Cycle Assessment
SSE	Sum of Square Errors
TES	Thermal Energy Storage tank
TES_{DHW}	TES for Heating/Cooling
TES_{HC}	TES for DHW
U value	Thermal transmittance (W/m^2K)
$\eta_{distributin}$	Efficiency of distribution systems
$\eta_{regulation}$	Efficiency of regulation systems
$\eta_{emission}$	Efficiency of emission systems

and guidelines, Green Building Rating Systems (GBRSs), and the methods developed by researchers in the literature. However, the previously published LCSA-related standards have delivered robust methodologies for evaluating the buildings' life cycle performance and will be used as the basis of LCA, LCC, and SLCA calculations in this paper; an integrated LCSA-based model to evaluate all three sustainability pillars is still a research gap [8]. An integrated approach can facilitate finding the balanced design scenarios from LCA, LCC, and SLCA perspectives simultaneously [8].

Although many research works have already been conducted to provide the frameworks of Life Cycle Assessment (LCA), Life Cycle Costing (LCC), and Social Life Cycle Assessment (SLCA) as the three LCSA pillars, the absence of a streamlined and integrated LCSA model into the building design process is still a barrier to employ it in decision-making and design process [8,18]. The complexity and dynamic nature of the building design process on the one hand [19,20], and the inherent complexity of LCSA [21,22], as well as existing ambiguity of the sustainability concept [23] on the other hand, are the main reasons for limited application of LCSA methods in building design process. Therefore, a streamlined, integrated LCSA approach is essential to facilitate LCSA implementation into buildings' design-assessment process.

Apart from established standards of building sustainability assessment frameworks and Green Building Rating Systems (GBRSs), various methods have been proposed and applied as individually developed methods in the literature. For instance, Amini Toosi & Lavagna [24,25] proposed a conceptual framework of integrating LCSA into energy retrofit design through a weighted-sum approach. In another study, Sherif, Tarek & Fahmy [26] developed a sustainability assessment tool for existing buildings based on experts' opinions. They proved that the relative importance of sustainability criteria varies from one country to another. A similar method is employed by Akhanova et al. [27] to provide a multi-criteria decision-making framework for building sustainability assessment. In a recent study, Janjua et al. [6] presented a methodology to choose Key Performance Indicators (KPIs) for sustainability assessment of residential buildings where the selection and weighting of KPIs are carried out based on literature review and the expert panels.

A recent review [8] revealed emerging trends in multi-dimensional LCSA studies. The cumulative number of multi-dimensional LCSA studies has been rapidly growing since 2011, and consequently, the application of optimization methods has increased. Table 1 presents recent LCSA-based building energy retrofitting studies by applying optimization methods and reports each paper's sustainability pillars' coverage. Among the papers published until 2020, those that addressed multiple LCSA pillars and applied optimization methods are summarized in Table 1.

The application of optimization methods in LCSA studies has emerged as a practical tool to overcome multi-criteria problem-solving complexity. While the Non-dominated Sorting Genetic Algorithm (NSGA-II) is known as the most popular algorithm, new methods based on Artificial Intelligence (AI) and Machine Learning (ML) are found as computational-time efficient solutions for performance-based design processes [8,28]. Artificial Neural Network (ANN), Support Vector Machine (SVM), and Gaussian Process Regression (GPR) have been the

Table 1
Sustainability pillars coverage and the employed optimization methods/algorithms in the recent building life cycle studies related to energy retrofit.

Authors, year	LCA	LCC	SLCA	Optimization algorithm
Chantrelle et al., 2011 [34]	✓	✓	✓	NSGA-II
Antipova et al., 2014 [35]	✓	✓	×	–
Carreras et al., 2015 [36]	✓	✓	×	NSGA-II
Carreras et al., 2016 [37]	✓	✓	×	–
Pal et al., 2017 [38]	✓	✓	×	NSGA-II
Ramin et al., 2017 [39]	✓	✓	×	–
Ylmén et al., 2017 [40]	✓	✓	×	NSGA-II
Mauro et al., 2017 [41]	×	✓	✓	NSGA-II
Mostavi, Asadi, & Boussaa, 2017 [42]	✓	✓	✓	HS Algorithm
Hester et al.,. 2018 [43]	✓	✓	×	Genetic, Unguided specification, Sequential specification
Jokisalo et al., 2019 [44]	✓	✓	×	NSGA-II
Sharif & Hammad, 2019 [45]	✓	✓	×	Artificial Neural Network, Machine Learning, NSGA-II
Hirvonen et al., 2019 [46]	✓	✓	×	NSGA-II

most frequently used supervised ML algorithms in the literature [29,30]. Machine Learning, as an application of Artificial Intelligence (AI), enables a system to learn from past experiences to predict future scenarios [31]. ML methods as data-driven techniques could be applied to predict buildings' energy consumption based on a set of existing data set (e.g., historical data or simulation-based data). The application of data-driven methods such as ML is rapidly growing in the field of building performance assessment, and many studies have already elaborated the state-of-the-art of this research field [29,31,32,33].

As shown in Table 1, LCA and LCC are considered in most papers, whereas few studies have taken SLCA-related indicators into account. Among those few articles, only thermal comfort is evaluated as an SLCA-related indicator. Almost all papers considered LCSA pillars separately and have optimized them individually. However, these multi-objective optimization methods help find the optimum solutions in the design process; they rarely guide the final optimum decision among a set of quasi-optimum scenarios. The main challenges in the previous methods and studies are the limited number of evaluated indicators related to LCSA pillars, the lack of a streamlined LCSA-based decision-making model, and the extensive computational time required for assessment.

A recent study conducted by Amini Toosi et al. [17] classified several challenges associated with life cycle sustainability assessment as a multi-criteria evaluation process in building and energy retrofit design. The lack of a transparent methodology to link and integrate the three LCSA pillars, harmonization of different metrics, the challenges of indicators' aggregation such as formulation, weighting, and normalization, and the extensive time required for data analysis and result processing are introduced as of the most persistent challenges in implementing LCSA into sustainable building and energy retrofit design [17].

In such a context, the present work proposes a streamlined LCSA-Machine learning-based optimization model applicable to the design process of new buildings and Energy Retrofit Measures (ERMs) of existing ones. Therefore, a novel model is developed to reach this goal by proposing a mathematical definition and formulation of life cycle sustainability assessment in compliance with EN standards for evaluating the environmental performance (EN 15978, 2011), economic performance (EN 16627, 2015), and social performance (EN 16309, 2014) of buildings. Supported by a set of interconnected equations, normalization, and weighting methods, the proposed LCSA-based model, can evaluate design scenarios' performance from an LCSA point of view and assign intermediate and final LCSA indices to each design scenario. These indices will be employed to compare the LCSA performance of the design scenarios within an optimization process coupled with Machine Learning (ML) methods to accelerate the data analysis and the optimization process. In the end, as a recommended solution to cope with the technical aspects of the built environment's electrification [14], the optimization of short-term Energy Storage Systems (ESSs) in an Italian residential building is chosen as an exemplary case study to show the proposed model's capabilities in building design process.

2. Methodology development

This section aims to propose an integrated LCSA-based model to be applied in the building design process. The model consists of mathematical definitions of LCSA criteria, including LCA, LCC, and SLCA performance in compliance with EN standards. Through a normalization method, the LCA, LCC, and SLCA indices will be defined as the intermediate indices of the model. Then, a general form of an aggregated final LCSA index will be presented by proposing a new weighting method and a weighted-sum approach. Fig. 1 illustrates the steps of the weighted-sum procedure for computing the final aggregated LCSA index. The weighted sum procedure starts with the definition of LCA impact categories, LCC parameters, and related impact categories of SLCA. Then as described within section 2.1 and in compliance with the EN standards, LCA, LCC, and SLCA indicators will be computed. Next,

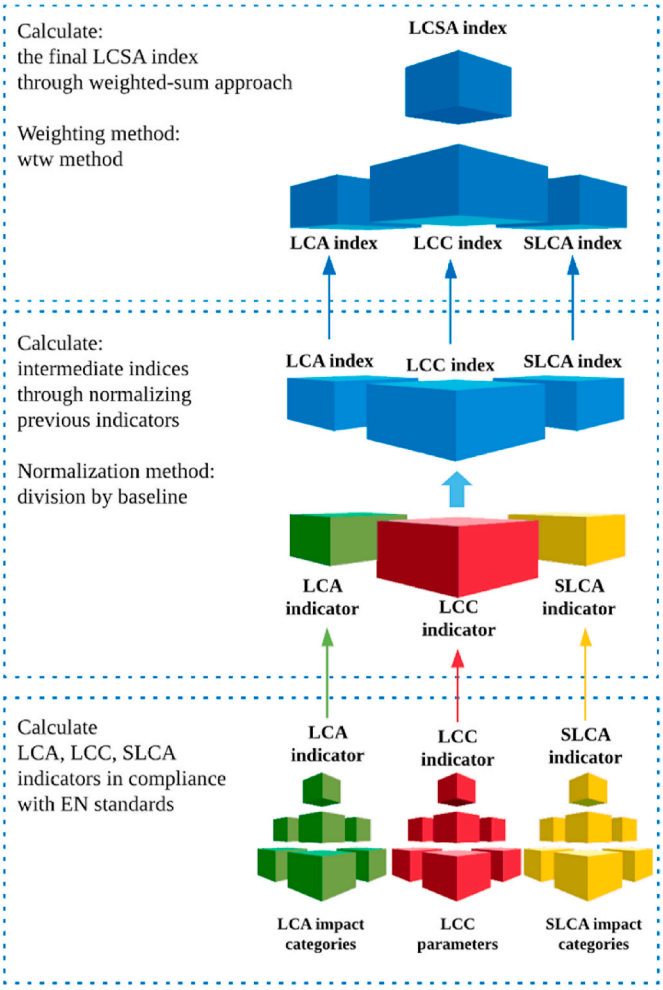

Fig. 1. Weighted-sum approach to calculate the LCSA final aggregated index.

LCA, LCC, and SLCA indicators will be normalized by a reference value as explained in section 2.1 to prepare the unitless LCA, LCC, and SLCA indices. Then, using the weighting method in section 2.2.1 and the new formulation of the final LCSA index in section 2.2.2, an aggregated LCSA index will be achieved for an overall life cycle sustainability assessment.

In the next step, a set of composite functions to provide a parametric form of the final LCSA index are proposed. The parametric form of the indices in which all influential building parameters are involved can support the parametric analyses. Then as described in section 2.3, to integrate the proposed LCSA based model into the design process, the model is coupled with Machine Learning (ML) models to accelerate the design-assessment process. The selection and implementation of ML models are described in section 2.3. This model could be applied in the LCSA-based optimum design process of new buildings and retrofitting scenarios of existing ones.

2.1. The mathematical definition of LCSA pillars: intermediate indices and normalization

In this section, the calculation steps of LCA, LCC, and SLCA indicators are explained. These indicators must be normalized to be applied in a weighted-sum approach for computing the final aggregated LCSA index. The normalization factors must be based on a known and available reference and should have a meaningful quantitative relation to the building's performance under study. Thus, division by baseline as an internal normalization method is taken in this step. The baseline could be defined as the Business as Usual model's performance (BAU) for new

building design or the pre-retrofit performance for retrofitting design.

2.1.1. LCA index

The LCA index is defined as a normalized index computed by Eq. (1) that shows the extent to which the design scenario has higher or lower environmental impacts than the baseline (BAU or pre-retrofit scenario). Values higher than one mean the design scenario has higher total environmental impacts than the baseline from an LCA perspective and vice versa.

Eq. (1) LCA index

$$LCA\ index_i = \frac{LCA\ indicator_i}{LCA\ indicator_{baseline}}$$

where:

LCA indicator represents the total aggregated environmental impacts of the design scenario over its life cycle phases. According to Ref. [47], it can be calculated using Eq. (2). If there is only one environmental impact category, the normalization by baseline scenario (Eq. (1)) and weighting method proposed in the final LCSA index formula (Eq. (5)) are sufficient. Otherwise, if more than one environmental impact category is taken into account, it is necessary to follow the optional LCIA steps of normalization and weighting to produce an aggregated LCA indicator to be used in Eq. (1).

Eq. (2) LCA indicator

$$LCA\ indicator_i = \sum_{i=A1}^{D} \sum_{j,k} W_j \frac{M_{ijk}}{N_j} (Q_{ik})$$

Where:

$\boldsymbol{W_j}$ is the weighting factor for the impact category j.

$\boldsymbol{N_j}$ is the normalization factor for the impact category j.

$\boldsymbol{M_{ijk}}$ is the quantity of impact of the impact category j, in the life cycle module i, caused by a unit of material and/or energy and/or activity k.

$\boldsymbol{Q_{ik}}$ is the quantity of material and/or energy and/or activity k, in life cycle module i, causing. M_{ijk}

Although normalization and weighting methods are optional steps in LCIA methods, these steps are considered mandatory in this model to assign a final aggregated LCA indicator to the design scenarios. Weighting (W_j) and normalization (N_j) factors in LCA are still open challenges. This model suggests taking the most reliable and updated values reported in LCIA guidelines if consistent with the adopted LCIA method. Some examples of these values are presented in Ref. [48,49,50]. The model is flexible to adopt different LCIA methods to calculate (M_{ijk}) provided by the relevant standards. Various environmental impact categories are suggested by LCA standards, such as Global Warming Potential, Ozone Depletion Potential, Acidification Potential, etc. [47]. This model can adopt all suggested impact categories and urges to follow the relevant standards to analyze the environmental impacts in this step.

2.1.2. LCC index

The index shows the extent to which the design scenario has higher or lower life cycle costs than the baseline scenario. A higher LCC index corresponds with a lower economic performance. Any LCC index values below 1 indicate that the evaluated design scenario has lower life cycle costs and better economic performance than the baseline. Eq. (3) formulates the LCC index.

Eq. 3 LCC index

$$LCC\ index_i = \frac{LCC\ indicator_i}{LCC\ indicator_{baseline}}$$

Where the *LCC indicator* should be selected according to the relevant standards [51,53], the standards already suggest some LCC indicators, such as Net Present Value (NPV) in Ref. [51] or payback period, net saving, Savings to Investment Ratio (SIR), and adjusted internal rate of return in Ref. [52]. However, this model can adopt different LCC indicators in either building retrofitting projects or new building designs; the value calculated for the baseline scenario's LCC indicator is not allowed to be zero or undefined. For example, suppose the baseline is defined as the pre-retrofit scenario. In that case, some LCC indicators are not applicable since they are equal to zero or undefined in the pre-retrofit scenario (e.g., net saving, SIR, payback time, etc.). While the baseline is defined as a BAU retrofitting plan, all suggested LCC indicators by the standards are applicable in this model.

2.1.3. SLCA index

According to the EN 15643-3 [53], social impact in SLCA is defined as any change to the society or the quality of life (adverse or beneficial) expressed with quantifiable indicators in the following categories: *Accessibility, Adaptability, Health, and Comfort, Loading on the neighborhood, Maintenance, Safety and Security, Sourcing of materials and services, Stakeholder involvement*. EN 15643-3 [53] has already provided the general SLCA framework, and the calculation methods for SLCA categories have been proposed by Ref. [54]. However, there are still several challenges in social impact assessment, such as the lack of consensus on social indicators [55], the choice of suitable SLCA indicators [56], the measurement, normalization, weighting, and aggregation of SLCA indicators [57].

A recent review study suggested that each indicator's relevance must be localized and justified in respective studies since they cannot be homogenized across all sectors and disciplines [58]. Likewise, we first propose choosing the most relevant SLCA categories according to each study's goal and scope and then taking a quantitative measurement method for each selected indicator. Our proposed model can adopt any quantitative SLCA indicator in the calculation process regarding the design project's goal and scope under evaluation.

Since the goal/scope and the relevant SLCA indicators are considered to be determined by the designer's perception, the binary weighting method in which the weights (W_j) are assigned according to the designer's opinion is selected as the appropriate weighting method among SLCA impact categories. Division on the baseline scenario is used as the normalization method for SLCA indicators to form the SLCA index (Eq. (4)). As already described for the previously proposed indices, the baseline scenario could be the BAU scenario for the new building design and the pre-retrofit scenario for the building retrofitting design.

Eq. (4) SLCA index

$$SLCA\ index_i = \sum_j W_j \left(\frac{SLCA\ indicator_j}{SLCA\ indicator_{j,\ baseline}} \right)$$

Where:

$\boldsymbol{SLCA\ indicator_j}$ is the quantitative indicator for SLCA impact category j.

$\boldsymbol{W_j}$ is the weighting factor for the impact category j.

Eq. (5) shows the general form of the SLCA index. This index shows the extent to which the design scenario has higher or lower performance compared to the baseline. A higher SLCA index means better SLCA performance, desirable in the design process.

2.2. The general form of the final LCSA index

Given the LCA, LCC, and SLCA indices proposed in the previous

sections, the final LCSA index will be defined through a weighted-sum approach. This index could be used in the comparative assessment of building products or building design scenarios. The mathematic definition and numerical results of the final LCSA index allow its application in a design-optimization process.

2.2.1. Weighting method

Weighting is a critical issue in multi-criteria decision-making [59]. Regardless of which weighting method is used, a critical associated risk of using weighting methods in the weighted-sum approach is that some weighting sets could lead to an unbalanced multi-criteria performance solution. It is known as the compensation issue in which the decrease of one index will be compensated by increasing another index. It happens when the maximum improvement of one index is remarkably lower than the others, and these indices do not behave similarly (e.g., increasing the first indicator requires a decrease in others). This phenomenon depends on the behavior of each index against input parameters and its potential improvement in the optimization process. The critical point is that this phenomenon is difficult to be predicted before running the optimization process and interpreting the results.

A three-step weighting method (**wtw** method) is proposed in this LCSA-based model to avoid the above-described risk. This method starts with an optional **w**eighting set (equal weighting), followed by the definition of **t**hresholds for each index, and ends with a final **w**eighting set.

The first weighting set is optional and is considered only to help graphical representation of the LCSA initial results before the thresholds assignment (e.g., see case study 2). The threshold for each index guarantees the desired improvement in each index. The threshold values could be defined according to either the regulations or the project's goals. These values could also be expressed as a percentage of the desired indices' improvement compared to the baseline performance or the maximum achievable value of each index. In this step, only those scenarios that satisfy all the thresholds will be kept to be processed in the final weighting step.

The final weighting step facilitates choosing the solution leading to the highest possible LCSA index out of the previously filtered scenarios. Since thresholds guarantee the desired indices' improvement, the model is flexible to adopt any weighting set in this step.

2.2.2. Final LCSA index

Given the proposed LCA, LCC, and SLCA indices, the adopted normalization method (division by baseline), and the proposed weighting method (wtw), the final aggregated index of LCSA will be calculated by Eq. (5).

Instead of a simple summation over the weighted indices, this model proposes summing the weighted square-roots of SLCA, LCA, and LCC indices in Eq. (5). This configuration of the LCSA equation promotes those scenarios with a better balance and harmony among all LCSA pillars (a constructive mathematic proof is provided in Appendix 1).

It should be reminded that the SLCA index is defined as a value aimed to be maximized. In contrast, LCA and LCC indices represent each scenario's environmental damages and monetary costs and need to be minimized. Therefore, the LCSA index in Eq. (5) will be maximized when the SLCA index tends to its maximum and LCA/LCC indices incline to their minimum values. LCSA index equal to 1 represents the baseline scenario's performance. An LCSA index higher than 1 shows the LCSA performance improvement compared to the baseline scenario and vice versa.

Eq. (5) LCSA index

$$\begin{aligned} LCSA\ index_i &= W_{slca}\sqrt{\left(\frac{SLCA\ index_i}{1}\right)} + W_{lca}\sqrt{\left(\frac{1}{LCA\ index_i}\right)} \\ &\quad + W_{lcc}\sqrt{\left(\frac{1}{LCC\ index_i}\right)} \\ &= W_{slca}\sqrt{\left(\frac{SLCA\ indicator_i}{SLCA\ indicator_{baseline}}\right)} \\ &\quad + W_{lca}\sqrt{\left(\frac{LCA\ indicator_{baseline}}{LCA\ indicator_i}\right)} \\ &\quad + W_{lcc}\sqrt{\left(\frac{LCC\ indicator_{baseline}}{LCA\ indicator_i}\right)} \end{aligned}$$

Where:

$\boldsymbol{W_{slca}}$, $\boldsymbol{W_{lca}}$ and $\boldsymbol{W_{lcc}}$ are weighting factors for SLCA, LCA, and LCC indices according to wtw method ($\boldsymbol{W_{slca}} + , \boldsymbol{W_{lca}} + \boldsymbol{W_{lcc}} = 1$)

$\boldsymbol{i}$ is the design scenario for which the LCSA index needs to be calculated.

2.3. A parametric form of the LCSA model; proposing composite functions to form the indices

In implementing the proposed LCSA-based model into a parametric design process, a set of mathematical equations could be found among design variables and each sustainability pillar's indicator/index. These equations could be mathematically complicated or straightforward depending on indicator behavior against variation of design variables.

This section aims to rewrite the above-proposed indices by using composite mathematic functions. Then for each design-assessment process, each function's unique form could be realized using regression/ML models. The final LCSA index is a composite function composed of the LCA, LCC, and SLCA functions. The LCA, LCC, and SLCA functions are merged to a final index by weighting and normalization values as described in section 2.2.

LCA, LCC, and SLCA indicators can be described as different functions of building design variables, the efficiency of energy systems, etc. For instance, there could be a mathematical definition of LCA composed of building energy consumption, environmental impacts of materials, building systems, energy flows (e.g., electricity or natural gas), service life span, etc. Likewise, the LCC and SLCA functions for a project can be defined according to its scope and system boundary.

The following equations present the general form of composite functions that can relate design variables to LCSA assessment criteria:

$$LCA\ index = \boldsymbol{f}_1\ (f\ (x, y \ldots n),\ x, y \ldots n)$$

$$LCC\ index = \boldsymbol{f}_2\ (f\ (x, y \ldots n),\ x, y \ldots n)$$

$$SLCA\ index = \boldsymbol{f}_3\ (f\ (x, y \ldots n))$$

$$LCSA\ index = \boldsymbol{f}_4\left(\boldsymbol{f}_1\ (f\ (x, y \ldots n),\ x, y \ldots n), \boldsymbol{f}_2\ (f\ (x, y \ldots n),\ x, y \ldots n), \boldsymbol{f}_3\ (f\ (x, y \ldots n)),\ W_{f1},\ W_{f2},\ W_{f3}\right)$$

Where:

$\boldsymbol{f}\ (\boldsymbol{x}, \boldsymbol{y} \ldots \boldsymbol{n})$, relates design variables to the operational energy performance (consumption/generation) $\boldsymbol{x}, \boldsymbol{y} \ldots \boldsymbol{n}$, are the design variable values $\boldsymbol{f_1}$ to $\boldsymbol{f_4}$ composite functions that relate design variables to LCA, LCC, SLCA, and LCSA indices, respectively. $\boldsymbol{W_{f1}}$, $\boldsymbol{W_{f2}}$, $\boldsymbol{W_{f3}}$ are the

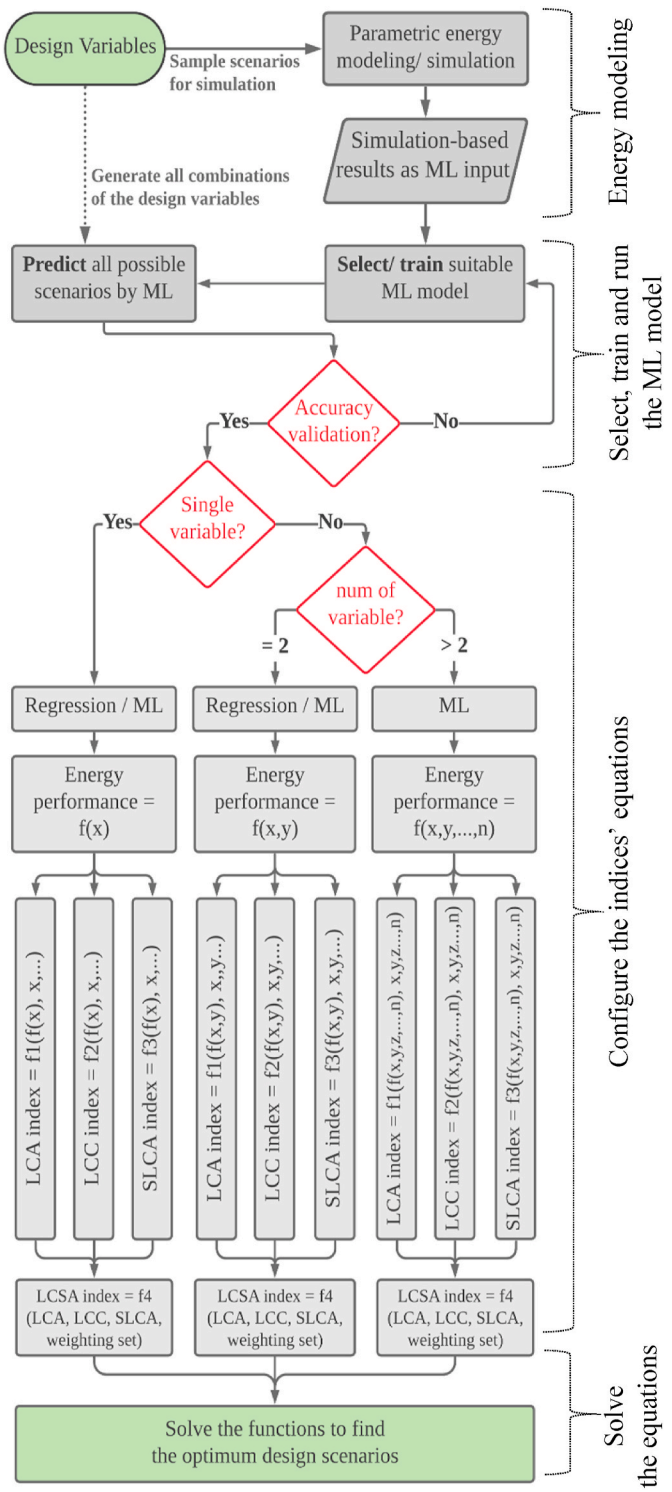

Fig. 2. Steps of implementing the proposed model in a parametric design/ assessment process.

weighting factors of LCA, LCC, and SLCA indices, respectively (according to wtw method).

To solve these composite functions, it is fundamental to present a unique form for f and f_1 to f_4. Regression analysis or ML methods can achieve the unique form of functions f and $f1$ to $f4$. Fig. 2 illustrates our proposed approach to defining these functions, starting by determining design variables followed by energy simulation and regression-based ML methods.

As shown in Fig. 2, the first step is to select the design variables. After running the parametric energy analysis for pre-selected design variables, a sufficient number of energy simulation results will be inserted in the ML process as inputs to predict the building energy performance for all possible design variable combinations. The adequate input number in the ML/regression model will be agreed upon when a perfect regression model is achieved within a trial-and-error process. The sufficient number of inputs depends on the parametric energy model's complexity, design variables, and ML algorithm efficiency. The more design variables and the more complicated relationship among design variables and indicators lead to more required inputs.

Among all ML models, Gaussian Process Regression (GPR) and Artificial Neural Network (ANN) are found as the commonly used and robust and efficient learning surrogate models for non-linear problem solving [30,60]. The efficiency and continuous application of these ML models in building energy performance predictions have been proved and reported in recent review studies [29,30,32,33,60]. To select the ML algorithm for different case studies, we recommend testing different algorithms and using the algorithm with the highest accuracy in each case study. The prediction accuracy of the ML model can be compared according to the coefficient of determination (R^2) [30]. The following case studies in this paper use a Gaussian Process Regression ML model to predict the design scenarios' performance.

The adequate number of inputs will train the selected ML model to enable it for results prediction. The predicted results should be compared to the results achieved by the simulation-based (non-ML) process to check if the ML model's accuracy is acceptable. After verifying the ML model's accuracy, all possible scenarios predicted by the ML model will be categorized based on the number of design variables. For instance, the energy consumption/performance could be defined as a single-variable polynomial function (f(x)) using regression analysis for a single variable optimization. Otherwise, it could be described as a two-variate function $f(x, y)$. If more than two variables are selected in the design-assessment process, we propose using a regression learning-based ML model instead of a polynomial function to realize $f(x, y, \ldots, n)$.

Then, unique forms of LCA, LCC, and SLCA functions could be solved using numerical methods to find the optimum design variables leading to maximum/minimum functions' values. Finally, using the LCA/LCC/SLCA functions, the LCSA function could be mathematically formed and solved to find the optimum results from an LCSA perspective.

2.4. Implementing the integrated LCSA-based model into the design process-requirements, limitations, and uncertainties

The first requirements are to define the goal, scope, and system boundary of the study. Thus, deciding what building life cycle modules must be included in the system boundary is required. However, it is recommended to take into account the whole life cycle phases (A1-D). Still, subject to the goal, the system boundary could be simplified to each case study's dominant life cycle modules. It should then be determined how buildings interact with the adjacent systems, including environmental, economic, and social contexts. Then, the building's services, components, materials, and energy flows in selected life cycle modules could be identified and included in the assessment. The selection of impact categories and indicators related to each sustainability pillar is still challenging. The model is flexible to adopt different impact categories and indicators for each sustainability pillar but recommends following the previously established EN standards [47,51,54].

At present, the model's main limitations and challenges are the choice of suitable SLCA indicators, the quantification method, and the aggregation of SLCA indicators. This model proposes considering the established impact categories by the relevant standards and is flexible to adopt new impact categories and indicators of all three sustainability pillars if provided by future research and standards.

The uncertainty of input data accuracy must be kept in mind as a significant issue. Almost all LCA, LCC, and SLCA input data will be

Fig. 3. Residential building, Bagnolo, Italy.

collected from external sources such as LCI databases, manufacturers' datasheets, governmental economic reports, etc. Consequently, low accuracy or limited access to reliable input data will increase the uncertainty of the results. It is paramount to use the most representative and well-known data resources to enhance the quality and reliability of results.

Although the proposed wtw-weighting method in this model guarantees a balanced design, the definition of thresholds and final weighting sets in this method might need external references to the social/economic and environmental programs' targets defined by external parties such as the governmental, international bodies, or other stakeholders. While it could be appreciated as the model's flexibility, it might be challenging when the thresholds are not defined by standards and depend on conflicting interests among stakeholders.

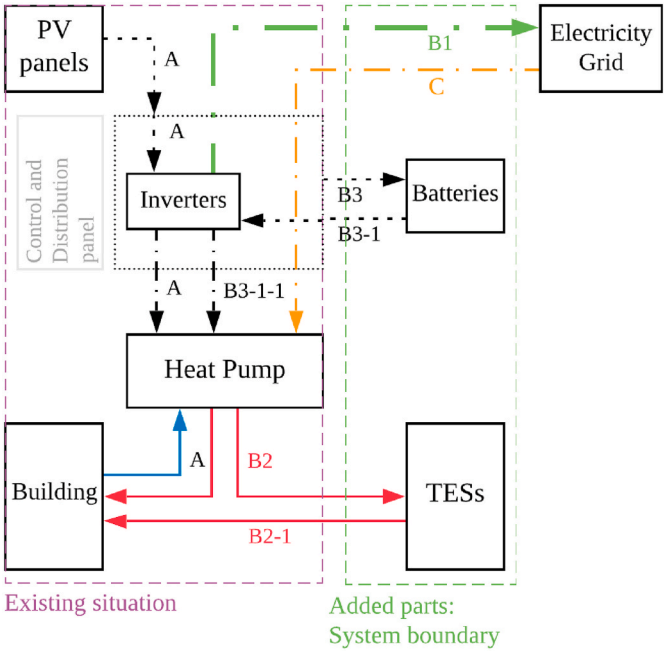

Fig. 4. Working scheme and system boundary, **A**: Direct use, **B1**: export to the grid (if excess PV > 0 and hourly need = 0), **B2**: thermal storage in TES (if excess PV, and hourly need >0), **B2-1**: Discharge TES, **B3**: Charge batteries (if TES is full, excess PV and need >0), **B3-1**: discharge batteries when PV is not enough and heat pump is in operation, **C:** import electricity from grid when PV and stored energy are lower than needs.

3. Exemplary case studies: implementation of the proposed model

An Italian residential building is chosen as the case study to test and verify the proposed LCSA-based model's capability. The case study is a multi-family house in Bagnolo in Piano, Reggio Emilia, Italy, constructed in 1985 (Fig. 3). It consists of four floors -including three residential floors-with an overall volume of 1900 m^3 and a net floor surface of 636 m^2 divided into 12 apartments with a window to wall ratio of 13%. It has a concrete structure, and the envelope is built with brick cavity walls and single glass-wood frame windows. The roof and floors are made of concrete and hollow brick structure.

The building is also the demo case of the Horizon 2020 HEART "Holistic Energy and Architectural Retrofit Toolkit" project and has been retrofitted during 2020 and 2021, installing new energy-efficient technologies. More in detail, the toolkit includes both envelope solutions (thermal insulation and windows) to reduce the thermal loads and HVAC/energy generation technologies (multicrystalline photovoltaic tiles, high-efficiency air-to-water heat pumps, low-temperature fan-coils, water tanks for thermal storage, and Li-Ion batteries) to ensure the energy efficiency and RES exploitation. The general scheme of the proposed technical system is represented in Fig. 4. The energy modeling in this case study is parametrically performed by EnergyPlus, using the grasshopper plugins.

3.1. The goal, scope, and system boundary of the case study

Six pillars have already been identified for decarbonizing the built environment, including zero-carbon electricity, electrification of the end uses, green synthetic fuels, smart power grids, materials efficiency, and sustainable land use [14]. A paradigm shift towards distributed and renewable energy generation, including the photovoltaic systems, is observable and indispensable in achieving decarbonization targets. Energy storage technologies, both in the short-term and long-term, are of those technologies supporting this transition. At the building level, one of the strategies toward decarbonization is to maximize on-site or

Table 2
Building and energy modelling parameters in the case study.

Parameters	Values
Internal Floors	U value = 1.18 W/m^2K
Ground Floor	U value = 3.49 W/m^2K
Roof	U value = 0.55 W/m^2K
External Walls	U value = 0.266 W/m^2K
Windows	U value = 1.2 W/m^2K, SHGC = 0.6
COP of HP units	= 0.001 (water_temp - Ext_temp+10)^2 - 0.17 (water_temp - Ext_temp+10)+10
$\eta_{distribution}$, $\eta_{regulation}$, $\eta_{emission}$	0.95
Inlet water temperature to HP units	15 °C
Outlet water temperature from HP units	35 °C in space heating mode, 10 °C in space cooling mode 45 °C in DHW mode
Heating demand	28884 kWh_{Th}
Cooling demand	10785 kWh_{Th}
DHW demand	13226 kWh_{Th}
Electricity demand	14320 kWh_{el}
The inverter efficiency	0.95
PV module efficiency	0.16
PV system losses (wiring, connections, etc.)	5%
PV size (Peak power)	8.5 kW_p
DoD $_{Li\text{-}ion\ battery}$	0.80
Safety factor for battery system losses	1.20
Thermal transmittance of TES walls	U value = 0.35 W/m^2K
TES size for heating/cooling	Variable (0–10000 L)
TES size for DHW	Variable (0–5000 L)
Battery Capacity	Variable (0–20 kWh)
Storage is designed for	1 day ahead
The building's service life and all Components' technical life span	30 years equal to the study period

Table 3
Environmental and economic input data for LCSA analysis.

	Environmental data								Economic data		
	GWP (kg CO_2 eq)	**ODP** (kg CFC-11 eq)	**AP** (mol H + Eq)	**EP** (kg P-Eq)	**POCP** (kg NMVOC-Eq)	**RU-m** (kg sb eq)	**RU-f** (MJ)	**LCA** indicator*	Prices and tariffs (€)	PIR	DR
TES component (1 L)	1.201	7.6E-8	6.8E-3	6.5E-4	5.2E-3	4.1E-5	16.9E-7	1.94E-10	300 + (TES volume in Liters/2)	2.1%	3.68%
Li-ion Battery (1 kWh)	3.785	3.24E-7	7.28E-2	8.14E-3	2.17E-2	6.7E-4	57.93	1.45E-3	420 €/kWh		
Electricity (1 kWh), Italian mix	4.26E-1	5.8E-8	2.29E-3	1.2E-4	9.72E-4	3.3E-6	6.8764	3.78E-8	0.18 € (p*) 0.10 € (s*)		
Normalization factors	5.79E13	1.61E8	3.83E11	5.06E9	2.08E11	4.39E8	4.5E14				

LCA indicator* expresses the total aggregated environmental impact through normalization and weighting (optional LCIA steps). (p*) and (s*) stand for the tariffs of purchasing the grid-supplied and selling the excess PV-supplied electricity.

nearby renewable energy production and self-consumption of the electrified buildings with the minimum exchange of energy with the grid by applying ESSs coupled with non-programmable RESs such as solar photovoltaic panels [14].

This case study aims to find the optimum size of thermal/electrical energy storage systems in the above-described building regarding the critical role of ESSs towards decarbonization targets. Therefore, the study's scope is limited to the size of the short-term Thermal Energy Storage tanks (TES) and electrical batteries. Fig. 4 illustrates the working scheme, components, and streams in the system boundary of this study. Assuming equal technical life span for the ESSs' components and the building study period (30 years), the replacement phase of ESSs is excluded from the study. It is also presumed that the component's residual values will compensate for the disposal costs at the end of the life phase.

In this case study, ESSs sizing is considered the second phase of designing ERMs while within the initial steps, it is assumed that the building envelope's thermal properties have been improved to the values shown in Table 2. It was also assumed that the air to water heat pump units and Photovoltaic (PV) panels have already been defined according to the annual heating, cooling, and DHW demand; more in detail, in the selected case-study building, two heat pumps with a rated thermal power of 25 kW each and a PV system of 8.5 kW_p were designed to meet buildings energy needs. The COP of heat pump units can be calculated using the equation in Table 3 according to the performance map of the components [61]. The operational temperature of thermal energy storage tanks is 35, 10, and 45 Celsius in heating, cooling, and domestic hot water, accordingly. The temperature drop in TESs due to thermal energy loss will be compensated by heat pump units. Table 2 summarizes the building's characteristics and energy modeling parameters .

Different ESSs sizes affect the building-grid interaction in terms of imported/exported electricity from/to the electricity grid. Therefore, only the TES size and battery size expressed in liters and kWh alongside the resulting imported/exported electricity between the building and grid are included in the system boundary (Fig. 4). It should be remarked that each litre of heated-up/cooled-down water stored in TES could be equalized to kWh of electricity consumed by heat pump units. The required electricity for heat pump operation is provided by PV when solar radiation is available. When PV generation is lower than electricity consumption, electricity needs to be imported from the grid. The storage is feasible when hourly PV generation is higher than hourly electricity consumption. In this case, two potential scenarios exist instead of exporting the excess PV generation to the electricity grid:

1. To force heat pump units to produce more thermal energy to be stored in TESs and consume the stored energy when the PV generation is not enough (e.g., at nights and on cloudy days). In this case, the excess PV generation must be exported to the grid if TESs are fully charged or the energy need is lower than the TESs capacity within the next 24 h.
2. To use the battery system as the secondary ESSs after charging TESs. In this case, the batteries will be charged if TESs are fully charged, and there is still hourly electricity demand due to insufficient hourly PV generation to operate heat pumps.

Both scenarios will decrease electricity purchasing from the grid and reduce the export of PV-generated electricity to the grid. Considering different tariffs of imported/exported electricity, these scenarios at an optimum ESSs size would be cost-beneficial and provide environmental benefits through maximum use of PV-generated electricity. It also reduces the load on local/national electricity grid infrastructures by decreasing the exported electricity to the grid.

3.2. LCSA input data: intermediate indicators, impact categories, and input parameters

To start defining the LCA, LCC, and SLCA indicators, first, it is necessary to determine the environmental impact categories, LCC parameters, and SLCA impact categories. To cover a wide range of environmental impacts, seven impact categories including Global Warming Potential (GWP), Ozone Depletion Potential (ODP), freshwater and terrestrial Acidification Potential (AP), freshwater Eutrophication Potential (EP), Photochemical Ozone Creation Potential (POCP), Resource Use (RU, minerals & metals, and fossils) are included. Related to the application of eq. (2), equal weighting among these impact categories is considered according to the recommendation for the EU context [62]. For the normalization of environmental impact categories, the proposed values in Ref. [48] are considered. To calculate the life cycle environmental impacts in Table 3, the ecoinvent v3.6 2019 and ILCD 2.0 2018 are used as the LCI database and the Life Cycle Impact Assessment methodology (LCIA) [63]. The values proposed in the JRC report [80] are adopted as the normalization factors for each environmental impact category to sum-up them together in a unitless LCA indicator.

In this paper, the baseline scenario for both case studies 1 and 2 is the scenario before installing the EESs where the building energy systems are fully electrified, and the LCA indicator is calculated based on environmental impacts of grid-supplied electricity, LCC is calculated based on the price of grid-supplied electricity, and the tariffs of sold PV-supplied electricity to the grid and SLCA is calculated according to building-grid interaction. In the baseline scenario, all excess PV-generated electricity is injected into the grid, and the hourly electricity demand is imported from the grid when the hourly PV-generated electricity is not enough to meet the building's demand. Therefore, in the baseline scenario, only the market of low-voltage Italian electricity mix is considered for the building's environmental impacts. In case study 1, hot water tank production (CH) is also considered to calculate the environmental impacts of thermal energy storage systems according

to ILCD 2.0 2018 in ecoinvent 3.6 2019. Moreover, in case study 2, the rechargeable Li-ion battery production (GLO) is also added to calculate the environmental impact of battery systems. The environmental impact of electricity and the EESs components are reported in Table 3. As a simplification, the values of TES and battery components' environmental impacts are divided on the reference component's capacity in LCI database. Therefore, TES and Li-ion battery components' environmental impacts are reported for 1 L and 1 kWh storage capacity, respectively (Table 3).

To calculate the LCC index, NPV is selected as described in section 3.1.2. The grid-supplied electricity price and the remuneration for the excess PV-supplied electricity to be exported to the grid are taken from a recent study in Italy [61]. Furthermore, the macroeconomic parameters such as energy Price Inflation Rate (PIR) and Discount Rate (DR) are retrieved and calculated from economic reports based on ten years' average data [64,65,66]. For the sake of simplicity, the hourly electricity tariffs for imported and exported electricity from and to the grid are considered constant, as reported in Table 3.

This example includes ESSs and building grid interaction (imported/exported electricity) in the system boundary (Fig. 4). An associated risk of one-site PV electrification of buildings is to increase exported electricity load to the grid when hourly PV generation is surplus than hourly energy (electricity) consumption in the building. Since power grids are generally designed according to the peak energy demand and not based on the peak exported electricity from prosumers to the grid, an expansion of excess hourly PV generation might lead to an overload on the national electricity grid [67]. This overload on the electricity grid might cause damages to the electricity grid and reduce the safety and security of the electricity infrastructures [68]. One solution to avoid this risk is to promote self-consumption by applying EESs in electrified buildings [14,69].

Therefore, given that *safety/security-security against interruptions of utility supply* has already been identified as an SLCA impact category in Ref. [54], the self-consumption of PV-generated electricity as an indicator of overload-mitigation is chosen as the SLCA indicator in paper. This indicator could be computed by Eq (6):

Eq. (6) SLCA indicator

$$SLCA\ indicator_j = \left(1 - \frac{\int hourly\_Exp\_PV_{generation,\ j}dt}{\int hourly\_PV_{generation}dt}\right)$$

Where:

$hourly\_Exp\_PV_{generation,\ j}$ is the hourly exported PV generation in (kWh) for the scenario j;

$hourly\_PV_{generation}$ is the hourly PV generation (kWh) by the installed PV panels.

SLCA indicator ranges between 0 and 1, where "0" means all PV-generated electricity is injected into the grid, and "1" means all PV generation is self-consumed in the building.

3.3. The parametric form of the LCSA model: configuration of equations

After defining the goal, scope, and the system boundary of the case study and providing the input parameters for intermediate indicators calculation (LCA, LCC, and SLCA indicators), it would be possible to continue configuring the composite functions for sustainability pillars as proposed in section 2.3.

To configure the final form of these functions, it is required to provide the functions that relate the design variables to the case study's operational energy performance. This case study is divided into two cases to conduct this step and show the proposed model's functionality with different design variables. In the first case, only two variables, including the TES sizes for heating/cooling (TES_{HC}) and Domestic Hot Water (TES_{DHW}), are taken into optimization. In the second case, the size of the electrical battery is included as the third design variable. After providing the polynomial functions relating design variables to operational energy performance, these functions will be used as the elements of the composite functions for LCA, LCC, and SLCA indicators and indices.

Table 4
Coefficients (with 95% confidence bounds).

Coefficients	f (x,y)	g (x,y)
p00	11410	11300
p10	−0.7888	−0.7998
p01	−2.413	−2.491
p20	0.0001257	0.0001285
p11	0.00005061	0.00004058
p02	0.001905	0.001944
p30	−1.039E-08	−1.13E-08
p21	−1.156E-08	−9.89E-09
p12	1.32E-08	1.53E-08
p03	−7.001E-07	−7.14E-07
p40	2.534E-13	3.65E-13
p31	2.064E-12	1.91E-12
p22	−3.968E-12	−4.11E-12
p13	8.007E-13	5.27E-13
p04	1.194E-10	1.22E-10
p50	6.968E-18	2.17E-18
p41	8.345E-17	−7.73E-17
p32	−1.38E-17	−1.18E-17
p23	5.607E-16	5.68E-16
p14	−5.49E-16	−5.32E-16
p05	−7.666E-15	−7.83E-15
	Goodness of fit:	Goodness of fit:
	SSE: 6.995e+05	*SSE: 7.22e+05*
	R^2: 0.9996	*R^2: 0.9996*
	Adjusted-R^2 R^2:0.9996	*Adjusted-R^2 R^2: 0.9996*
	RMSE: 11.68	*RMSE: 11.86*

3.3.1. Case study 1: multi (two) variables optimization (TES_{HC} and TES_{DHW})

According to the steps illustrated in Fig. 2, the energy simulation is carried out using parametric energy analysis. A GPR-Machine learning model is used to predict all possible scenarios (including all allowed capacities of TES_{HC} and TES_{DHW} in liters). Then through the regression analyses (curve fitting), the building's energy performance functions are realized. In this case study, equations (7) and (8) and the values in Table 4 present as the energy performance functions and can be considered as the surrogate models of energy simulations by which the designer will be enabled to realize the electricity consumption and excess PV generation more rapidly without advanced prior knowledge in energy simulation. Equation (7) ***f(x,y)*** relates the x and y correspondingly as TES_{HC} and TES_{DHW} to the annual electricity demand (imported from the grid in kWh). Similarly, ***g(x,y)*** in equation (8) relates the annual excess PV generation to be exported to the grid in kWh. Then these functions are used to configure the functions of LCA, LCC, SLCA, and LCSA indices as presented by equations (9)–(12).

Eq. (7) Required annual electricity to be imported from the grid in kWh (***f(x,y)***)

$$\boldsymbol{f}(\boldsymbol{x},\boldsymbol{y}) = p00 + p10.x + p01.y + p20.x^2 + p11.x.y + p02.y^2 + p30.x^3 + p21.x^2.y + p12.x.y^2 + p03.y^3 + p40.x^4 + p31.x^3.y + p22.x^2.y^2 + p13.x.y^3 + p04.y^4 + p50.x^5 + p41.x^4.y + p32.x^3.y^2 + p23.x^2.y^3 + p14.x.y\hat{4} + p05.y\hat{5}$$

Eq. 8 Excess annual PV-generated electricity to be exported to the grid in kWh (***g(x,y)***)

$$\boldsymbol{g}(\boldsymbol{x},\boldsymbol{y}) = p00 + p10.x + p01.y + p20.x^2 + p11.x.y + p02.y^2 + p30.x^3 + p21.x^2.y + p12.x.y^2 + p03.y^3 + p40.x^4 + p31.x^3.y + p22.x^2.y^2 + p13.x.y^3 + p04.y^4 + p50.x^5 + p41.x^4.y + p32.x^3.y^2 + p23.x^2.y^3 + p14.x.y\hat{4} + p05.y\hat{5}$$

Where:

$\boldsymbol{f}(\mathbf{x},\mathbf{y})$ *is the anuual* needed electricity from the grid in kWh (to buy)

$\boldsymbol{g}\ (\boldsymbol{x},\boldsymbol{y})$ *is the annual* excess electricity to grid in kWh (to sell)

$\boldsymbol{x}$ is the TES size for heating/cooling in liters.

$\boldsymbol{y}$ is the TES size for DHW in liters.

Therefore, the equations of LCA, LCC, and SLCA indicators could be expressed as the following composite functions:

Eq (9) LCA indicator

$$\textbf{LCA } indicator = \boldsymbol{f}_1(\boldsymbol{f}(\boldsymbol{x},\boldsymbol{y}),\boldsymbol{x},\boldsymbol{y}) = f(x,y) \times env\_impact_{electricity} \times s + (x+y) \times env\_impact_{TES}$$

Eq (10) LCC indicator

$$\textbf{LCC } indicator = \boldsymbol{f}_2(\boldsymbol{f}(\boldsymbol{x},\boldsymbol{y}),\boldsymbol{g}(\boldsymbol{x},\boldsymbol{y}),\boldsymbol{x},\boldsymbol{y}) = NPV(f(x,y)) - NPV\ (g(x,y)) + (x+y) \times TES\_price$$

Eq (11) SLCA indicator

$$\textbf{SLCA } indicator = \boldsymbol{f}_3(\boldsymbol{g}(\boldsymbol{x},\boldsymbol{y})) = 1 - \left(\frac{g(x,y)}{\int hourly\_PV_{generation}dt}\right)$$

Where

this case study is the pre-retrofit scenario before installing TESs. Then the LCSA index is defined and calculated by the following Eq. (12).

Eq (12) LCSA index

$$\textbf{LCSA index} = W_{lca}\sqrt{\left(\frac{1}{LCA\ index}\right)} + W_{lcc}\sqrt{\left(\frac{1}{LCC\ index}\right)} + W_{slca}\sqrt{\left(\frac{SLCA\ index}{1}\right)}$$

$$= \boldsymbol{f}4(\boldsymbol{f}_1(\boldsymbol{f}(\boldsymbol{x},\boldsymbol{y}),\boldsymbol{x},\boldsymbol{y}),\ \boldsymbol{f}_2(\boldsymbol{f}(\boldsymbol{x},\boldsymbol{y}),\boldsymbol{g}(\boldsymbol{x},\boldsymbol{y}),\boldsymbol{x},\boldsymbol{y}),\ \boldsymbol{f}_3(\boldsymbol{g}(\boldsymbol{x},\boldsymbol{y})),W_{LCA},W_{LCC},W_{SLCA})$$

$$= W_{lca}\sqrt{\left(\frac{f_1(f(x_0,y_0),x_0,y_0)}{f_1(f(x,y),\ x,y)}\right)} + W_{lcc}\sqrt{\left(\frac{f_2(f(x_0,y_0),\ g(x_0,y_0),\ x_0,y_0)}{f_2(f(x,y),\ g(x,y),\ x,y)}\right)} + W_{slca}\sqrt{\left(\frac{f_3(g(x,y))}{f_3(g(x_0,y_0))}\right)}$$

Where:

$\boldsymbol{W_{LCA}}$, $\boldsymbol{W_{LCC}}$, $\boldsymbol{W_{SLCA}}$ *are the weighting factors* (will be employed according to wtw method)

$\boldsymbol{env\_impact_{electricity}}$ *is the total environemtal impacts of* 1 *kWh electricity provided by the grid* (*table* 3)

$\boldsymbol{env-impact_{TES}}$ *is the total envoronmental impacts of TES component with* 1 *Liter capacity* (*table* 3)

$\boldsymbol{x_0,\ y_0}$ refers to the baseline scenario $\left(\text{in this case}, \boldsymbol{x}_{0,}\ \boldsymbol{y}_0 = 0\right)$

$$\textbf{NPV}\ (\boldsymbol{f}(\boldsymbol{x},\boldsymbol{y}))\ is\ Net\ Present\ Value\ of\ f(x,y) = \sum_{s=0}^{s-1} f(x,y)(El\_P_1)\left(\frac{1+PIR_1}{1+DR}\right)^s$$

$$\textbf{NPV}\ (\boldsymbol{g}(\boldsymbol{x},\boldsymbol{y}))\ is\ Net\ Present\ Value\ of\ g(x,y) = \sum_{s=0}^{s-1} g(x,y)(El\_P_2)\left(\frac{1+PIR_2}{1+DR}\right)^s$$

x and y *are the size of TES for heating / cooling and domestic hot water* (*liters*)

s *is the study period* (*table* 3)

3.3.2. Case study 2: multi (three) variables optimization (TES_{HC}, TES_{DHW}, and battery)

In this case study, the size of a Lithium-ion battery system is added to the design variables to store PV-generated electricity when excess PV generation exists. The priority of storage is given to the thermal energy storage; therefore, the battery is charged only when the TESs are fully charged and the need for electricity in the next 24 h exists. Fig. 5 illustrates the control logic of thermal-electrical energy storage systems.

In this case, three design variables are included in the LCSA-based optimization process. Therefore the aforementioned functions of energy performance could be expressed as ***f(x,y,z)*** and ***g(x,y,z),*** where x, y, and z stands for the size of TES_{HC}, TES_{DHW}, and the battery capacity,

$\boldsymbol{El\_P_1}$ *it the price of electricuty to buy from the grid* (*Euro per kWh*) *presented in table* 3

$\boldsymbol{El\_P_2}$ *it the price of electricuty to sell to the grid* (*Euro per kWh*) *presented in table* 3

PIR *is the annual energy price inflation rate* (*table* 3)

DR *is the discount rate* (*table* 3)

TES_price *is the price of the TES for each* 1 *Liter storage capacity* (*table* 3)

Then, according to the model described in section 2.1, LCA, LCC, and SLCA indices are computed by dividing each scenario's LCA, LCC, and SLCA indicators over the baseline scenario's indicators. The baseline in

respectively. As already proposed in Fig. 2, in the case studies with more than two design variables, an ML model is recommended to find the relation between design variables and energy performance. Therefore, instead of the polynomial functions, A Gaussian Regression Process ML model will predict and produce the results of all possible variables' combinations. Finally, LCA, LCC, SLCA indicators, and LCSA index are expressed in equations (13)–(16) where ***f(x,y,z)*** and ***g(x,y,z)*** stands for the ML models that predict the required grid-supplied electricity and the excess PV-generated electricity in kWh respectively.

Eq (13) LCA indicator

$$\textbf{LCA indicator} = f_1(f(x,y,z),x,y,z) = f(x,y,z) \times env\_impact_{electricity} \times s + (x+y) \times env\_impact_{TES} + z \times env\_impact_{Battery}$$

Eq (14) LCC indicator

$$\textbf{LCC indicator} = f_2(f(x,y,z),g(x,y,z),x,y,z) = NPV(f(x,y,z)) - NPV(g(x,y,z)) + (x+y) \times TES.price + z \times Battery.price$$

Eq (15) SLCA indicator

$$\textbf{SLCA indicator} = f_3(g(x,y,z)) = 1 - \left(\frac{g(x,y,z)}{\int hourly\_PV_{generation}dt}\right)$$

Then according to the general definition of LCSA index:
Eq (16) LCSA index

$$\textbf{LCSA index} = W_{lca}\sqrt{\left(\frac{1}{LCA\ index}\right)} + W_{lcc}\sqrt{\left(\frac{1}{LCC\ index}\right)} + W_{slca}\sqrt{\left(\frac{SLCA\ index}{1}\right)}$$

$$= f_4(f_1(f(x,y,z),x,y,z), f_2(f(x,y,z),g(x,y,z),x,y,z), f_3(g(x,y,z)), W_{LCA}, W_{LCC}, W_{SLCA})$$

$$= W_{LCA}\sqrt{\left(\frac{f_1(f(x_0,y_0,z_0),x_0,y_0,z_0)}{f_1(f(x,y,z),\ x,y,z)}\right)} + W_{LCC}\sqrt{\left(\frac{f_2(f(x_0,y_0,z_0),\ g(x_0,y_0,z_0),\ x_0,y_0,z_0)}{f_2(f(x,y,z),\ g(x,y,z),\ x,y,z)}\right)} + W_{SLCA}\sqrt{\left(\frac{f_3(g(x,y,z))}{f_3(g(x_0,y_0,z_0))}\right)}$$

Where:

$\textbf{env\_impact}_{electricity}$ *is the total environmental impacts of* 1 *kWh electricity provided by the grid* (*table* 3)

$\textbf{env\_impact}_{TES}$ *is the total environmental impacts of the TES with* 1 *Liter storage capacity* (*table* 3)

$\textbf{env} - \textbf{impact}_{Battery}$ *is the total environmental impacts of the battery system with* 1 *kWh storage capacity* (*table* 3)

$$\textbf{NPV}\ (f(x,y,z))\ is\ Net\ Present\ Value\ of\ f(x,y) = \sum_{s=0}^{s-1} f(x,y)(El\_P_1)\left(\frac{1+PIR}{1+DR}\right)^s$$

$$\textbf{NPV}\ (g(x,y,z))\ is\ Net\ Present\ Value\ of\ g(x,y) = \sum_{s=0}^{s-1} g(x,y)(El\_P_2)\left(\frac{1+PIR}{1+DR}\right)^s$$

x, y *and* z *are the TESs size for heating / cooling, and DHW* (*liters*) *and the battery capacity* (*kWh*)

s *is the service life span* (*table* 3)

El_P_1 *it the price of electricity to buy from the grid* (*Euro per kWh*) *presented in table* 3

El_P_2 *it the price of electricity to sell to the grid* (*Euro per kWh*) *presented in table* 3

PIR *is the annual energy price inflation rate* (*table* 3)

DR *is the discount rate* (*table* 3)

TES_price *is the price of the TES for each* 1 *Liter storage capacity* (*table* 3)

$Battery_{price}$ *is the price of the battery for each* 1 *kWh storage capacity*

W_{LCA} , W_{LCC} , W_{SLCA} *are the weighting factors*

x_0, y_0 , z_0 *refers to the pre − retrofit baseline scenario* ($=0$)

3.4. Results and discussion

The results of exemplary case studies are presented and discussed in two following sections according to the methodology developed in the previous sections for case study 1 with two design variables and case study 2 with three design variables.

Each case study is discussed separately, and the optimum solutions of the EESs sized are reported according to LCA, LCC, SLCA, and final aggregated LCSA indices. By comparing the results, the performance and accuracy of implementing the Machine Learning algorithm is discussed, and the performance of the proposed LCSA-Machine Learning-based optimization model is highlighted.

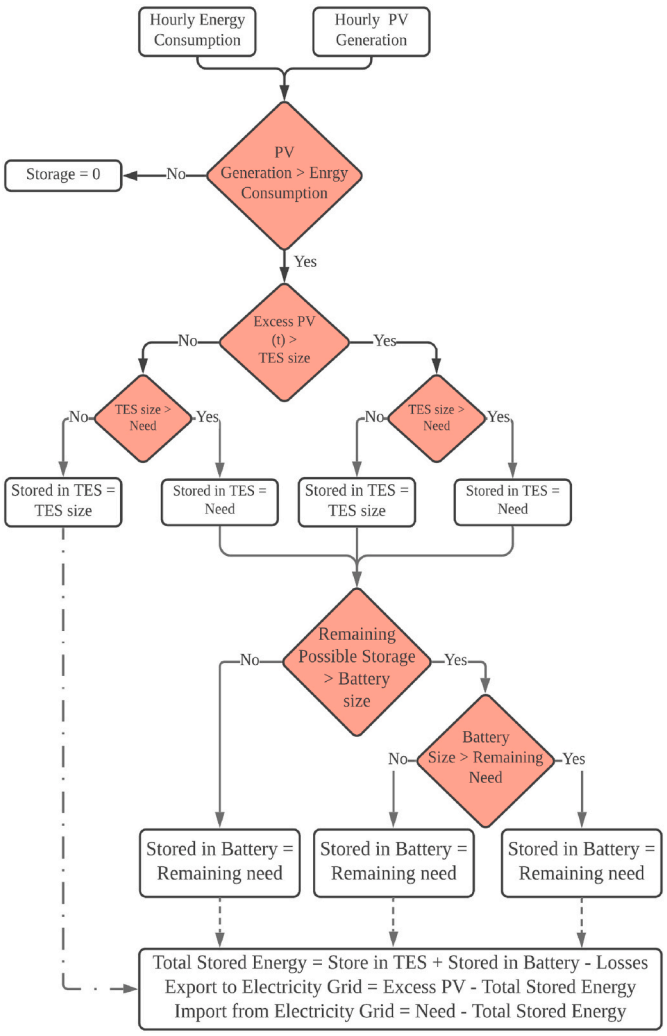

Fig. 5. Control logic of ESSs scheme work priority.

3.4.1. *Results in case study 1: LCSA-based optimization for TES_{HC} and TES_{DHW}*

The optimization of the TESs size for heating/cooling and domestic hot water is performed using the materials and methods described in the previous sections. To select the suitable ML algorithm, the prediction accuracy of different available algorithms in Matlab machine-learning toolbox are compared according to the coefficient of determinations, and Gaussian Process Regression (GPR) algorithm representing a perfect R^2 equal to 1, is selected and employed to predict all possible scenarios' performance (various TESs sizes). The application of the ML model resulted in significant computational time and power saving. The following heat graphs (Figs. 6–8) present LCA, LCC, and SLCA indices for different TESs sizes. Then using the wtw weighting method, the LCSA index is also computed, and the results are presented in Figs. 9 and 10.

As shown in Fig. 6, the lowest LCA index representing the best environmental performance occurs when the TES size for heating/cooling and DHW are 3800 and 900 L, respectively. This scenario's LCA index is reduced to 0.840, representing almost 16% improvement compared to the baseline scenario. This is the maximum achievable improvement in LCA performance by installing ESSs in the building case study. The dotted area in Fig. 6 shows the scenarios by which at least 50% of the maximum possible improvement (8%) could be achieved. This area includes all the design scenarios in which the LCA index is lower than 0.9195 (LCA_index threshold).

Similarly, according to Fig. 7, the best economic performance is obtained when the TES size for heating/cooling and DHW are 3100 and 900 L, respectively. This scenario decreases the LCC index to 0.868 and provides almost 13.2% maximum possible improvement in LCC performance than the pre-retrofit baseline scenario. LCC index in this case study is the most sensitive index to TES sizes' variation due to its contingency of being highly affected adversely or slightly beneficial. The dotted area in Fig. 7 represents the scenarios in which the LCC index is lower than 0.934 (LCC_index threshold), corresponding to 50% of the maximum achievable improvement in LCC performance. Figs. 6 and 7 show that the LCA and LCC indices increase sharply for large TES sizes. This sharp increase in LCA and LCC indices can be explained by the fact that in the scenarios with huge TES sizes, the extra capacity of the TES will never be in operation and therefore does not benefit the building in reducing energy consumption, costs, and environmental impacts of the operational phase. In contrast, it directly increases the costs and embodied environmental impacts of the installed ESSs.

The SLCA index behaves differently and shows a continuous and progressive improvement by increasing TES sizes for heating/cooling and domestic hot water. This behavior is explicable since the increase of TES size results in less electricity export to the grid. Therefore, as shown in Fig. 8, the highest SLCA index corresponding to the best SLCA performance occurs at the maximum allowed size of TESs. SLCA index can

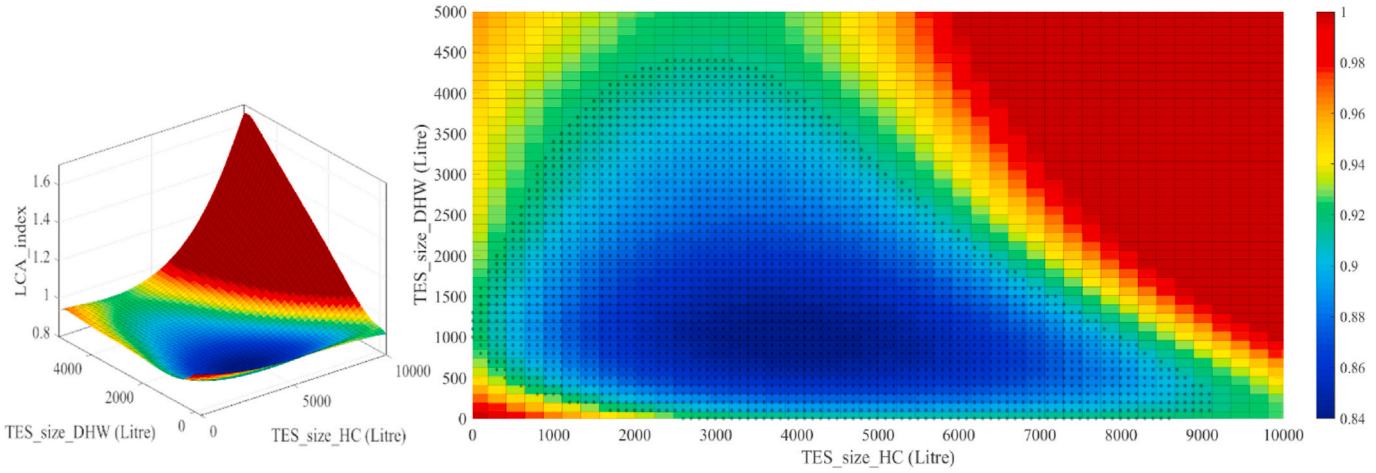

Fig. 6. Results of LCA index for different combination of TES sizes, the colors represent the value of LCA index. Lower LCA index (dark blue) means better LCA performance. The dotted area represents the scenarios with at least 50% of the maximum achievable LCA index improvement (LCA_index threshold). (For interpretation of the references to color in this figure legend, the reader is referred to the Web version of this article.)

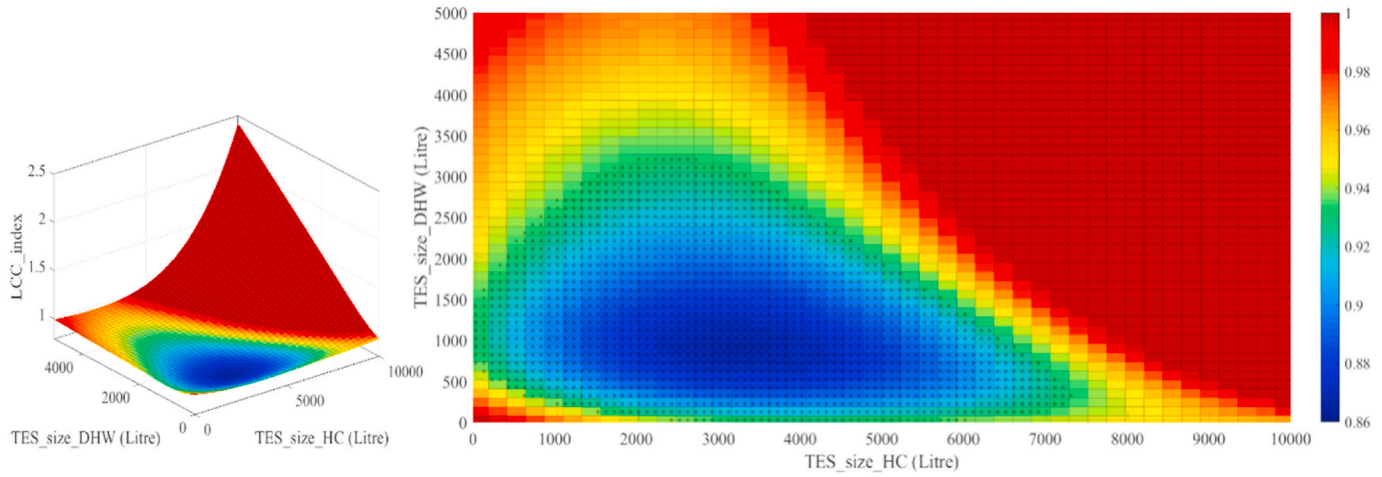

Fig. 7. Results of LCC index for different combination of TES sizes, the colors represent the value of LCC index. Lower LCC index (dark blue) means better LCC performance. The dotted area represents the scenarios with at least 50% of the maximum achievable LCC index improvement (LCC_index threshold).

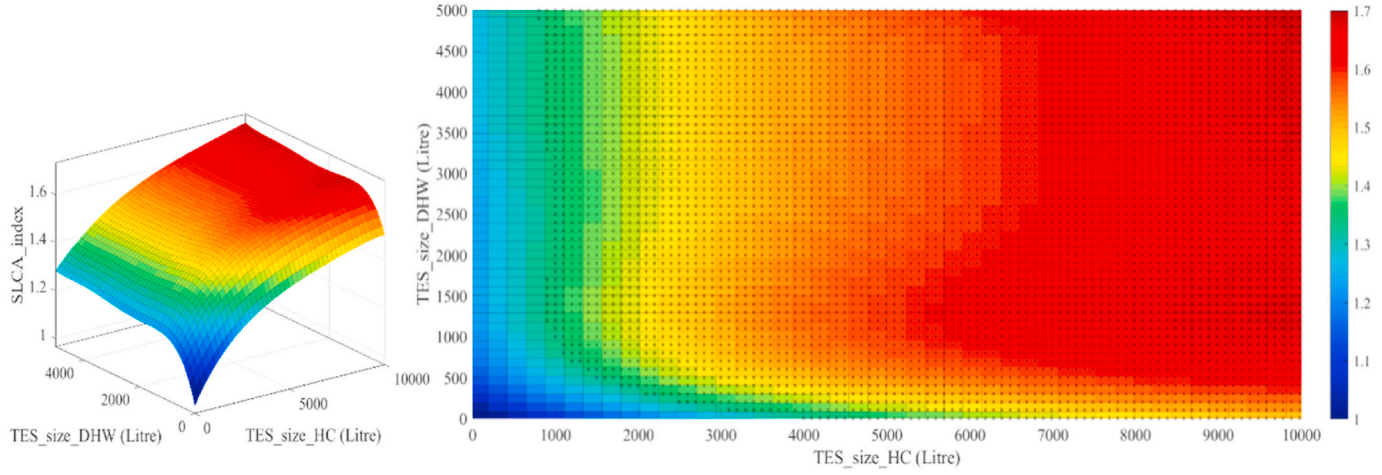

Fig. 8. Results of SLCA index for different combination of TES size, the colors represent the value of SLCA index, Higher SLCA index (dark red) means better SLCA performance. The dotted area represents the scenarios with at least 50% of the maximum achievable SLCA index improvement (SLCA_index threshold). (For interpretation of the references to color in this figure legend, the reader is referred to the Web version of this article.)

reach the value of 1.697, corresponding to 69.7% improvement when the TES size of heating/cooling and DHW are 10000 and 5000 L. However, as shown in previous figures, LCA and LCC indices in this scenario have lower performance compared to the pre-retrofit baseline scenario. Like previous indices, the dotted area with at least 50% of the maximum possible SLCA improvement (SLCA_index >1.3488) is shown in Fig. 8.

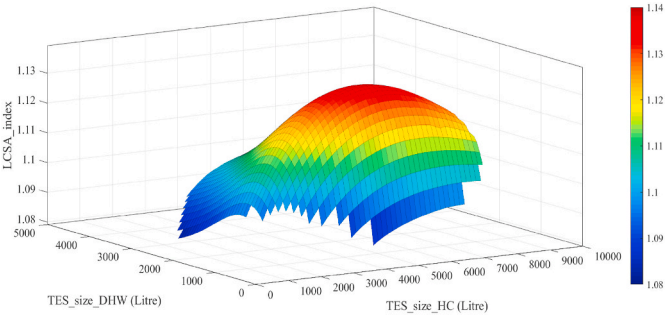

Fig. 9. Three dimensional view of the LCSA index's results versus different TES sizes. Higher index value (dark red) corresponds with higher LCSA performance. wtw method is used as the weighting method as described in the text. (For interpretation of the references to color in this figure legend, the reader is referred to the Web version of this article.)

While the decision-making is straightforward to choose the optimum TES size according to each index, the different behavior of LCA, LCC, and SLCA indices brings complexities to the decision-making when all three indices are set as the optimization targets.

To resolve this complexity and avoid the risk of an unbalanced design, as already described in section 2.2.1 a new weighting method is used. To use wtw weighting method and provide a single LCSA index, it is required to define the desired thresholds of LCA, LCC, and SLCA performance first. Then set of weighting factors for all three indices will be applied according to the project's targets and priorities.

In this case, it is assumed that all three indices must be improved at least to 50% of their maximum achievable performance as the desired indices' thresholds (the dotted area in Figs. 6–8 and 10). Therefore, the thresholds are 0.9195, 0.9340, and 1.3488 for LCA, LCC, and SLCA indices accordingly. Figs. 9 and 10 represent the LCSA index results for all combinations of design variables that satisfy the thresholds. Since this case study is presented just as an application of the model and does not intend to make a value-choice decision on LCSA pillars, equal weighting factors are also applied in the last step of wtw weighting

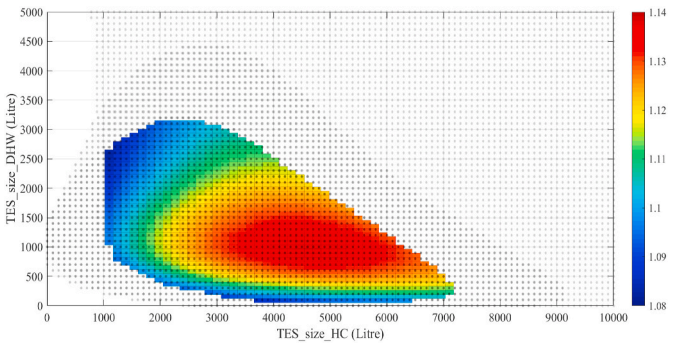

Fig. 10. Two dimensional view of the LCSA index's results versus different TES sizes. Higher index value (dark red) corresponds with higher LCSA performance. wtw method is used as the weighting method as described in the text. The LCSA optimum results are located in the overlapping dotted areas in which LCA, LCC and SLCA index are improved at least 50% of their maximum achievable improvement. (For interpretation of the references to color in this figure legend, the reader is referred to the Web version of this article.)

method to calculate the final LCSA index. As shown in Fig. 10, the LCSA results are constrained in the overlapping area of LCA, LCC, and SLCA thresholds.

The colors in Figs. 9 and 10 show the LCSA index's values. As illustrated in these figures, the final optimum TES sizes for heating/cooling and DHW are 4500 and 1000 L, where the highest LCSA index equal to 1.1364 is achieved. This optimum scenario leads 13.64% improvement in LCSA performance compared to the pre-retrofit scenario's performance. It also results in 15.8, 12, and 57.4% improvement in LCA, LCC, and SLCA indices equivalent to 98.22, 91.03, and 82.28% of the maximum achievable improvement in LCA, LCC, and SLCA indices, respectively. Table 5 summarizes the optimum scenarios' results from LCA, LCC, SLCA, and LCSA perspectives.

These results confirm that the proposed LCSA-based model can efficiently find the balanced optimum solution concerning all three LCSA pillars by which the LCSA index is maximized, and all LCA, LCC, and SLCA performance are improved significantly. It should be noted that this method can find the highest LCSA performance and provide the results of all possible scenarios to inform the designers with the required information to choose quasi-optimum solutions.

Given the relation between design variables and operational energy consumption, there are two methods to configure the indices' equations: 1) applying regression analysis and creating polynomial functions and 2) the machine learning methods to realize the correlation among design variables and operational energy performance of the scenarios. Both methods are proven to be highly accurate; however, it is necessary to adopt machine learning with higher accuracy for case studies with more than two design variables or a complicated relationship between design variables and energy performance.

In this case study, the prediction accuracy of the polynomial functions and GPR-ML model as the surrogate models for energy simulations are compared for 100 random scenarios and shown in Figs. 11 and 12. By comparing the relative errors in Figs. 11 and 12, it is perceived that both f(x,y) and g(x,y) are predicted with the same accuracy level, although by comparing the two surrogate models, the GPR-ML model provided a significantly higher accuracy in predicting the results of both f(x,y) and g(x,y) functions.

The relative error reveals to what extent the predicted results by regression analysis are lower or higher than the simulation results. As shown in Figs. 11 and 12, the maximum absolute error in predicting f(x,y) and g(x,y) by polynomial functions are 2.82% and 2.85%, while the maximum absolute error of predicted results by machine learning is considerable lower equal to 0.132% and 0.138% for f(x,y) and g(x,y) respectively. Likewise, the mean absolute relative error of the predicted results by polynomial functions equals 0.218% and 0.221%. The application of machine learning to predict f(x,y) and g(x,y) has the mean absolute error equal to 0.010 and 0.011 that represents a significant accuracy.

Although both methods provide a high level of accuracy, it is paramount to use machine learning as the most accurate method since minor errors in prediction might affect the final optimum solutions in some cases. In this case study, the optimum scenarios predicted by polynomial composite functions were presented first. However, the user is encouraged to apply machine learning to configure the indices' equations. The final results by application of machine learning are shown in Table 6.

The optimum results shown in Table 5 are more accurate and reliable due to the higher accuracy of machine learning in predicting f(x,y) and g(x,y). The difference between optimum results presented in Table 5 and Table 6 lies in the different accuracy between the prediction by GPR-machine learning model and linear regression analysis applied to form polynomial functions in this case study. Both methods to configure f(x,y) and g(x,y) have pros and cons. Although implementing polynomial functions to realize f(x,y) and g(x,y) is nearly accurate, straightforward, and does not require prior knowledge of machine learning, implementing machine learning enhances the model's performance and results' precision significantly. Furthermore, although the results in Table 6 highlight only the LCA, LCC, SLCA, and LCSA benefits of installing the energy storages systems coupled with heat pump units and photovoltaic panels, it is worthy of mentioning that the LCSA-based optimum size of energy systems in this case study, has also resulted in 24.27% reduction in grid-supplied electricity consumption.

3.4.2. *Results in case study 2: LCSA-based optimization for TES_{HC} and TES_{DHW} and battery size*

Following the similar steps in the first case study and by implementing the configured equations presented in section 3.3.2 for case study 2, the LCA, LCC, and SLCA indices for each combination of design variables (different scenarios) are calculated. Then, through the application of the wtw weighting method, the final LCSA index for each scenario is computed, and all results are presented in Figs. 13 and 14. These figures display a different form of results presentation necessary in case studies with more than three variables. In those cases, the three-dimensional graphs in which the indices' values are displayed on the graph's axes are the most informative and comprehensive form of results' presentation. Each point in Figs. 13 and 14 represents one possible combination of variables as a scenario. The colors represent the value of the LCSA index of the scenarios. In Fig. 13, equal weighting for LCA, LCC, and SLCA indices is employed to compute the LCSA index (the first optional step of wtw method).

Table 5
The summary of optimum results in case study 1.

	ESSs Size		Index value				The improvement compared to the baseline (%)			
	TES_{HC} (Liters)	TES_{DHW} (Liters)	LCA_index	LCC_index	SLCA_index	LCSA_index	LCA	LCC	SLCA	**LCSA**
Baseline (pre-retrofit)	0	0	1	1	1	1	–	–	–	**-**
LCA_optimum	3800	900	0.84	0.871	1.543	1.1352	16	12.9	54.3	**13.52**
LCC_optimum	3100	900	0.842	0.868	1.51	1.1308	15.8	13.2	51	**13.08**
SLCA_optimum	10000	5000	1.67	2.428	1.697	0.9065	−67	−142.8	69.7	**−9.35**
LCSA_optimum	**4500**	**1000**	**0.842**	**0.88**	**1.574**	**1.1364**	**15.8**	**12**	**57.4**	**13.64**

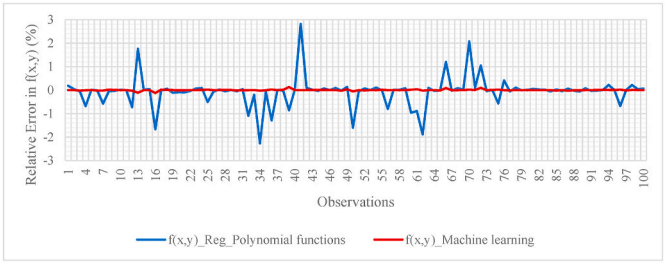

Fig. 11. The relative error of the results of f(x,y) predicted by polynomial functions and machine learning. SD of results by polynomial functions = 0.619 SD of results by GPR-machine learning = 0.028.

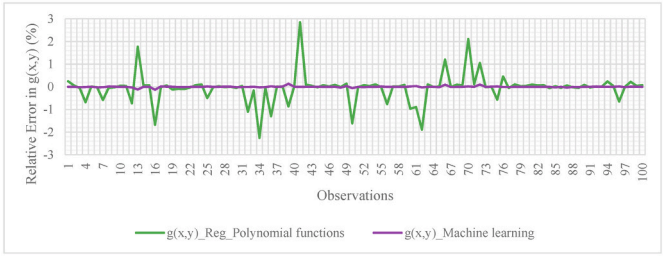

Fig. 12. The relative error of the results of g(x,y) predicted by polynomial functions and machine learning. SD of results by polynomial functions = 0. 623SD of results by GPR-machine learning = 0.029.

The optimum ESSs sizes from an LCA perspective are found equal to 1900 L, 600 L, and 20 kWh for TEShc, TESdhw, and the battery, respectively. Likewise, regarding the LCC index, the design variables' optimum values are 3500, 1000, and 0 for TES_{hc}, $TES_{dhw,}$ and the battery accordingly. The SLCA index behaves differently; it is found that the maximum allowed size of ESSs leads to the heights SLCA index. Therefore 10000 L, 5000 L, and 20 kWh are seen as the optimum design variables regarding the SLCA index; however, they adversely affect the LCA and LCC index. Table 7 summarizes the results of optimum scenarios for all indices and shows their relative improvements concerning the baseline scenario and the maximum achievable performance of each index.

As proposed in the wtw weighting method, to select the LCSA-optimum scenario, first, the indices' thresholds are applied to guarantee the desired level of improvement in all three LCA, LCC, and SLCA indices. Similar to the previous case study, the thresholds are defined as 50% of each index's maximum achievable improvement. Therefore, the thresholds are equal to 0.8987, 0.9578, and 1.2983 for LCA, LCC, and SLCA indices.

Fig. 14 represents the scenarios located in the thresholds box, where the scenarios satisfy all indices' thresholds. Following the third step of the wtw method and using equal weighting among LCA, LCC, and SLCA indices, the final LCSA index's values are computed to be compared and find the final optimum scenario.

The optimum design variables are equal to 6000, 1000 L, and 0 kWh for TES_{hc}, $TES_{dhw,}$ and the battery accordingly. In this scenario, the LCSA index is 1.0994, leading to 9.94% improvement compared to the baseline. It also results in 11.1, 7.1, and 44.1% improvement in LCA, LCC, and SLCA index. Moreover, the LCSA-based optimum results reduced the consumption of grid-supplied electricity by 24.27% compared to the baseline scenario in which no EESs is installed.

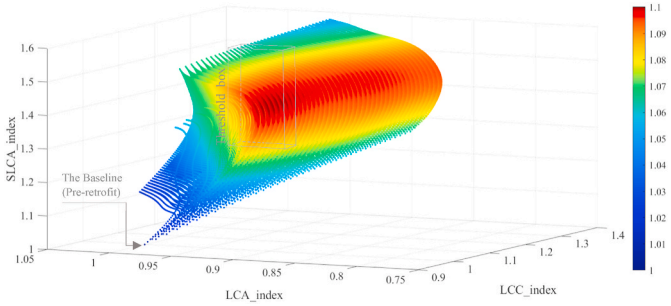

Fig. 13. Results of LCSA index for all possible scenarios, colors represent the value of LCSA index based on equal weighting (1st step of wtw weighting method). Each dot shows a possible scenario of ESSs size combination. The threshold box contains those scenarios that satisfy the thresholds of all indices. (For interpretation of the references to color in this figure legend, the reader is referred to the Web version of this article.)

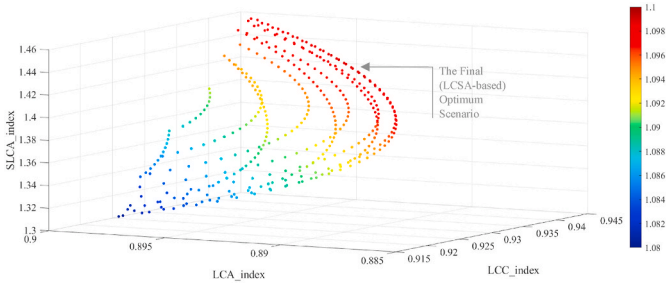

Fig. 14. LCSA results of the scenarios within the thresholds box. Colors represent the value of LCSA index based on 3rd step of wtw weighting method (described in the text). The dark red color represents the scenarios with highest achievable LCSA index as the final optimum solution. (For interpretation of the references to color in this figure legend, the reader is referred to the Web version of this article.)

Two reasons explain why the electrical battery application is not found among optimum solutions from LCC, and LCSA viewpoints in case study 2. First, in this study, it is assumed that the ESSs are designed only to provide thermal energy demand and not to support the electrical appliances' energy consumption. Therefore, the immediate use of the excess PV-generated electricity to be stored as thermal energy in TESs is a more efficient solution than the battery charge/discharge cycle. Secondly, the electrical battery system is considered as the secondary energy storage strategy. Therefore, since the priority in energy storage scheme-works is given to thermal energy storage (TESs), The low energy storage potential after charging TESs is insufficient to justify the high battery systems' costs.

Given the results in case studies 1 and 2, it is possible to compare the

Table 6
The summary of optimum results in case study 1 predicted by GPR-ML model.

	ESSs Size		Index value				The improvement compared to the baseline (%)			
	TES_{HC} (Liters)	TES_{DHW} (Liters)	LCA_index	LCC_index	SLCA_index	LCSA_index	LCA	LCC	SLCA	**LCSA**
Baseline (pre-retrofit)	0	0	1	1	1	1	–	–	–	-
LCA_optimum	4400	1000	0.884	0.918	1.4	1.0969	11.6	8.2	40	**9.69**
LCC_optimum	3500	1000	0.886	0.915	1.368	1.0924	11.4	8.5	36.8	**9.24**
SLCA_optimum	10000	5000	0.993	1.073	1.506	1.0654	0.7	−7.3	50.6	**6.54**
LCSA_optimum	**6000**	**1000**	**0.889**	**0.929**	**1.441**	**1.0994**	**11.1**	**7.1**	**44.1**	**9.94**

Table 7
The summary of optimum results in case study 2.

	ESSs Size			Index value				The improvement compared to the baseline (%)			
	TES_{HC} (Liters)	TES_{DHW} (Liters)	Battery (kWh)	LCA_index	LCC_index	SLCA_index	LCSA_index	LCA	LCC	SLCA	**LCSA**
Baseline (pre-retrofit)	0	0	0	1	1	1	1	–	–	–	**-**
LCA_optimum	1900	600	20	0.798	1.127	1.478	1.0925	21.2	−12.7	47.8	**9.25**
LCC_optimum	3500	1000	0	0.887	0.915	1.368	1.0924	11.3	8.5	36.8	**9.24**
SLCA_optimum	10000	5000	20	0.949	1.338	1.596	1.0514	5.1	−33.8	59.6	**5.14**
LCSA_optimum	**6000**	**1000**	**0**	**0.889**	**0.929**	**1.441**	**1.0994**	**11.1**	**7.1**	**44.1**	**9.94**

accuracy of the ML-based prediction against the polynomial functions obtained by a curve-fitting regression-based forecast of the energy performance. Since the electrical storage was not found as the LCSA optimum solution, both case studies' optimum results are expected to show the same optimum solutions and indices. However, different solutions and indices' values were found in these case studies (see Tables 5 and 7). Whereas, if the same ML model is used to predict the energy performance functions in case studies 1 and 2, similar results would be achieved for both cases since the accuracy of the predictive models is the same (see Tables 6 and 7).

This difference in results shown in Tables 5 and 7 for LCC and LCSA optimum solutions is caused by the different precisions of the predictive models used to configure energy performance functions in these case studies that were analyzed and discussed in section 3.4.1. In the first case study, $f(x,y)$ and $g(x,y)$ were formulated as polynomial functions of degree five while a more accurate ML model to predict $f(x,y,z)$ and $g(x,y,z)$ were employed in the second case study. The main advantage of the first case with lower accuracy is its straightforward application. In this case, once the polynomial functions are realized, the designer would be able to use them without previous advanced knowledge or the need for ML models. In contrast, the ML model will achieve higher accuracy in the second case to predict the energy performance functions for the indices' calculation. The difference between these two methods' accuracy depends on the complexity of energy performance functions' behavior against the design variables. Our study recommends using an ML-based model to predict energy performance functions if a complex correlation exists between design variables and energy performance.

4. Conclusion

In this paper, following a review and clarification of the methodological gaps in the literature, a novel LCSA-ML based model is proposed to design new buildings and building retrofitting. All three sustainability pillars are described mathematically by providing mathematic equations and respecting the existing standards. Then three intermediate indices covering LCA, LCC, and SLCA are provided. A final life cycle sustainability (LCSA) index is then defined through a weighted-sum approach using a new weighting method to guarantee the balance among intermediate indices.

The proposed LCSA model is also structured to be integrated into the optimization-based design process. Machine learning is integrated into the proposed model to facilitate the design/assessment process by reducing computational time and power and preserving its accuracy. Eventually, to provide an example of the model functionality, the model is tested in designing short-term Energy Storages Systems (ESSs) of an Italian residential building. The results showed that our proposed model application could effectively optimize the ESSs size from an LCSA perspective. The model is flexibly designed to be employed in designing all building types in different environmental, economic, and social contexts. The proposed model demonstrated its capability to facilitate the LCSA application in the sophisticated building design and assessment processes by delivering an efficient method and providing precise and tangible results. The results could be shared readily with designers and stakeholders who might not be LCSA experts.

The main model's limitations lie in the SLCA impact assessment and input data collection. The selection of SLCA impact categories/indicators and environmental data availability in the building sectors is still challenging; however, ongoing and future research projects are expected to resolve them. In this model, we proposed to choose SLCA indicators according to each case study's goal and scope. It could also be described as the model's flexibility since each project may target or encompass different social aspects. The model is flexibly designed to adopt new impact categories and indicators for all sustainability pillars if the future standards and studies deliver more robust quantitative indicators in LCSA. It should be stated that the application of the model is not limited to the exemplary case studies in this paper, and it could be applied in more diverse building design projects.

The model integration into new design/assessment tools could be suggested as a future research objective to expand its application for all building designers and engineers.

Declaration of competing interest

The authors declare that they have no known competing financial interests or personal relationships that could have appeared to influence the work reported in this paper.

Acknowledgment

This study and project are financially supported by EU Research and Innovation programme Horizon 2020 through number 768921 – HEART. The authors would like to thank the European Commission for enabling the funding of this project.

Appendix 1

This section provides a mathematical (constructive) proof of two statements that support why instead of simple summation of intermediate indices (LCA, LCC, and SLCA indices), we proposed summing up the square roots of intermediate indices to formulate the final aggregated index.

- 1st statement: If all intermediate indices are equal and similarly weighted and simply summed up, in case one index decreases and the other one increases equally; the results of the simple weighted sum will remain constant (compensation problem)
- 2nd statement: If the square roots of intermediate indices are similarly weighted and summed up, then the scenario with more harmony among intermediate indices results in a higher final aggregated index (helps avoid the compensation problem). This statement would be mathematically

approved if we can conclude that the final aggregated index will be maximized when the values of all intermediate indices are equal (perfect balance).

Therefore, assume:

- $\bullet \frac{1}{LCA_{index}} = a$,
- $\bullet \frac{1}{LCC_{index}} = a$,
- $SLCA_{index} = a$
- Weighting factor = w

Then, in the 1st case (simple summation: equal indices):

$$LCSA_{index} = w\left(\frac{1}{LCA_{index}}\right) + w\left(\frac{1}{LCC_{index}}\right) + wSLCA_{index} = 3wa$$

Let us assume that the value x decreases one inde***x*** and the other is increased equally.

- $\frac{1}{LCA_{index}} = a - x$,
- $\bullet \frac{1}{LCC_{index}} = a + x$,
- $SLCA_{index} = a$

in 2nd **case** (simple summation and unequal indices): simple summation of intermediate indices:

$$LCSA_{index} = w\left(\frac{1}{LCA_{index}}\right) + w\left(\frac{1}{LCC_{index}}\right) + wSLCA_{index} = w(a - x) + w(a+x) + wa = 3wa$$

Obviously, $+x$ and $-x$ could be crossed out. Therefore, the result of the $LCSA_{index}$ is equal to case 1, where all indices were equal. It simply shows that the decrement of one indicator is fully compensated by increasing the other index. (*Statement 1 is approved by comparing the results of case 1 and case 2*).

The compensation problem must be resolved. In other words, the different combination of intermediate indices must not result in an equal final aggregated index, and the case with better balance among indices should be promoted by receiving a higher final index. For this purpose, we proposed our new formulation of the final aggregated LCSA index by summing up the square roots of indices. Therefore, in case 3, we continue to verify the 2nd statement that supports our new formula of the final aggregated index.

In 3rd **case** (sum up square roots of unequal indices): Now, regarding our new formula in which the summation of square roots of intermediate indices are considered in formulating the final aggregated index:

$$LCSA_{index} = w\left(\sqrt{\frac{1}{LCA_{index}}}\right) + w\left(\sqrt{\frac{1}{LCC_{index}}}\right) + w\left(\sqrt{\frac{SLCA_{index}}{1}}\right) = w\left(\sqrt{(a - x)}\ w\sqrt{(a+x)} + \sqrt{a}\right)$$

Therefore:

$$(LCSA_{index})^2 = w^2\left(\sqrt{\frac{1}{LCA_{index}}} + \sqrt{\frac{1}{LCC_{index}}} + \sqrt{\frac{SLCA_{index}}{1}}\right)^2$$

$$= w^2\left(\sqrt{(a - x)} + \sqrt{(a+x)} + \sqrt{a}\right)^2$$

$$= w^2\left[\underbrace{[(a - x) + (a + x) + a]}_{\text{Constant phrase } =3a} + 2\underbrace{\left[\left(\sqrt{a(a - x)}\right) + \left(\sqrt{(a - x)(a+ x)}\right) + \left(\sqrt{a(a + x)}\right)\right]}_{\text{f(x)=Promoting phrase}}\right]$$

The second phrase is called the promoting phrase and is a function of ***x***. Since the first phrase is constant, to maximize the LCSA index, f(x) as the promoting phrase must be maximized.

The promoting phrase (***f(x)***) is the difference between case 2 and case 3 and depends on the value of ***x***. If the maximum value of the promoting phrase occurs at x = 0, we can conclude that this phrase will promote those scenarios in which LCA, LCC, and SLCA indices are balanced.

Therefore, let us find the extremum value of f(x):

$$\frac{df(x)}{dx} = \frac{d\left[\left(\sqrt{a(a-x)}\right) + \left(\sqrt{(a-x)(a+x)}\right) + \left(\sqrt{a(a+x)}\right)\right]}{dx} = 0$$

$\rightarrow x_{extermum} = 0$, then. $f(x_{extermum}) = 3a$

(The 2nd statement is approved since the maximum value of the promoting phrase is found at x = 0).

The boundaries of f(x) are:

$$if\ x \leq -a,\ then\ f(x) = not\ defined$$

$$if\ x = -a,\ then\ f(x) = a\sqrt{2}$$

$$x_{extermum} = 0,\ then\ f(x_{extermum}) = 3a$$

$$if\ x = a,\ then\ f(x) = a\sqrt{2}$$

$$if\ x \geq a,\ then\ f(x) = not\ defined$$

As illustrated in Fig A1, the promoting phrase's value decreases by increasing the value of $\boldsymbol{x}$. The boundary values of f(x) show that f(x) as the promoting phrase will be maximized when x = 0 indicates that the LCSA index will be maximized when a harmony among indices exists. It approves our statement that despite the simple summation of intermediate indices, summing up the square roots of intermediate indices will increase when a harmony among indices exists (x = 0); therefore, the scenario with a better balance among all indices will be promoted.

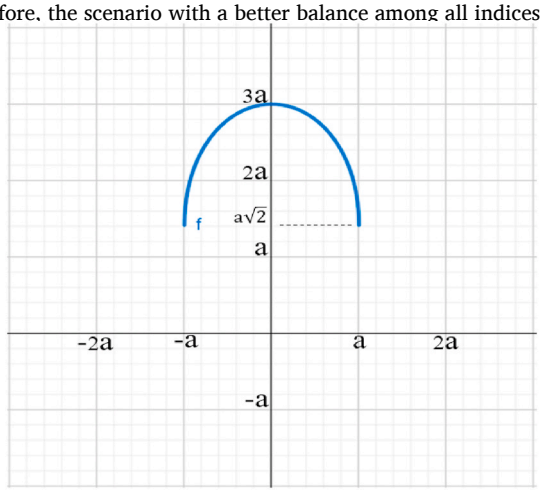

Fig. A.1. The graph of f(x).

References

[1] Yin Sin Lim, Bo Xia, Skitmore Martin, Jason Gray, Adrian Bridge, Education for sustainability in construction management curricula, Int. J. Constuct. Manag. 15 (4) (2015) 321–331, https://doi.org/10.1080/15623599.2015.1066569.

[2] UNEP, "Global alliance for buildings and construction, 2018 global status report", p. 325, 2018, doi: https://doi.org/10.1038/s41370-017-0014-9.

[3] R. Mateus, S.M. Silva, M.G. De Almeida, Environmental and cost life cycle analysis of the impact of using solar systems in energy renovation of Southern European single-family buildings, Renew. Energy 137 (2019) 82–92, https://doi.org/10.1016/j.renene.2018.04.036.

[4] N. Aste, P. Caputo, M. Buzzetti, M. Fattore, Energy efficiency in buildings: what drives the investments? The case of Lombardy Region, Sustain. Cities Soc. 20 (Jan. 2016) 27–37, https://doi.org/10.1016/J.SCS.2015.09.003.

[5] N. Mirabella, M. Röck, M. Ruschi Mendes Saade, C. Spirinckx, M. Bosmans, K. Allacker, A. Passer, Strategies to improve the energy performance of buildings: a review of their life cycle impact, Buildings 8 (8) (Aug. 2018) 105, https://doi.org/10.3390/buildings8080105.

[6] S.Y. Janjua, P.K. Sarker, W.K. Biswas, Development of Triple Bottom Line Indicators for Life Cycle Sustainability Assessment of Residential Buildings, vol. 264, November 2019, p. 2020.

[7] United Nations Environmental Program (UNEP), Note 12: towards a Life Cycle Sustainability Assessment, 2011. DTI/1412/PA.

[8] H. Amini Toosi, M. Lavagna, F. Leonforte, C. Del Pero, N. Aste, Life cycle sustainability assessment in building energy retrofitting; A review, Sustain. Cities Soc. 60 (Sep. 01, 2020) 102248, https://doi.org/10.1016/j.scs.2020.102248. Elsevier Ltd.

[9] E. Parliament, DIRECTIVE 2002/91/EC OF THE EUROPEAN PARLIAMENT AND OF THE COUNCIL of 16 December 2002 on the energy performance of buildings, Off. J. Eur. Commun. (2003) 65–71.

[10] E. Parliament, DIRECTIVE 2006/32/EC OF THE EUROPEAN PARLIAMENT AND OF THE COUNCIL of 5 April 2006 on energy end-use efficiency and energy services and repealing Council Directive 93/76/EEC, Off. J. Eur. Union (2006) 64–85.

[11] E. Parliament, DIRECTIVE 2010/31/EU OF THE EUROPEAN PARLIAMENT AND OF THE COUNCIL of 19 May 2010 on the energy performance of buildings, Off. J. Eur. Union (2010) 13–35.

[12] M. Paleari, M. Lavagna, A. Campioli, The assessment of the relevance of building components and life phases for the environmental profile of nearly zero-energy buildings: life cycle assessment of a multifamily building in Italy, Int. J. Life Cycle Assess. 21 (2016) 1667–1690, https://doi.org/10.1007/s11367-016-1133-6.

[13] A. Vilches, A. Garcia-Martinez, B. Sanchez-Montañes, Life cycle assessment (LCA) of building refurbishment: a literature review, Energy Build. 135 (Jan. 2017) 286–301, https://doi.org/10.1016/J.ENBUILD.2016.11.042.

[14] SDSN & FEEM, Roadmap to 2050: A Manual for Nations to Decarbonise by Mid-century, September, 2019.

[15] M. Finkbeiner, E.M. Schau, A. Lehmann, M. Traverso, Towards Life Cycle Sustainability Assessment, 2010, pp. 3309–3322, https://doi.org/10.3390/su2103309.

[16] J. Guinée, Life cycle sustainability assessment: what is it and what are its challenges? in: R. Clift, A. Druckman (Eds.), Taking Stock of Industrial Ecology Springer, 2015, pp. 45–68, https://doi.org/10.1007/978-3-319-20571-7.

[17] H. Amini Toosi, M. Lavagna, F. Leonforte, C. Del Pero, N. Aste, Implementing life cycle sustainability assessment in building and energy retrofit design—an investigation into challenges and opportunities, in: S.S. Muthu (Ed.), Life Cycle Sustainability Assessment (LCSA), Environmental Footprints and Eco-design of Products and Processes, Springer, Singapore, 2021, pp. 103–136. https://doi.org/10.1007/978-981-16-4562-4_6.

[18] C. Visentin, A. William, and A. B. Braun, "Life cycle sustainability assessment: a systematic literature review through the application perspective, indicators, and methodologies", J. Clean. Prod., vol. 270, 2020, doi: 10.1016/j.jclepro.2020.122509.

[19] A. Hollberg, J. Ruth, LCA in architectural design—a parametric approach, Int. J. Life Cycle Assess. 21 (7) (2016) 943–960, https://doi.org/10.1007/s11367-016-1065-1.

[20] E. Meex, A. Hollberg, E. Knapen, L. Hildebrand, G. Verbeeck, Requirements for applying LCA-based environmental impact assessment tools in the early stages of building design, Build. Environ. 133 (2018) 228–236, https://doi.org/10.1016/j.buildenv.2018.02.016. January.

[21] A. Invidiata, M. Lavagna, E. Ghisi, Selecting design strategies using multi-criteria decision making to improve the sustainability of buildings, Build. Environ. 139 (2018) 58–68, https://doi.org/10.1016/j.buildenv.2018.04.041.

[22] D. Costa, P. Quinteiro, A.C. Dias, A systematic review of life cycle sustainability assessment: current state, methodological challenges, and implementation issues, Sci. Total Environ. 686 (2019) 774–787, https://doi.org/10.1016/j.scitotenv.2019.05.435.

[23] S. Roostaie, N. Nawari, C.J. Kibert, Sustainability and resilience: a review of definitions, relationships, and their integration into a combined building assessment framework, Build. Environ. 154 (2019) 132–144, https://doi.org/10.1016/j.buildenv.2019.02.042. March.

[24] H. Amini Toosi, M. Lavagna, Life Cycle Sustainability Assessment (LCSA) and Optimization Techniques. A conceptual framework for integrating LCSA into designing energy retrofit scenarios of existing buildings, in: The 12th Italian LCA Network Conference. Life Cycle Thinking in Decision Making for Sustainability: from Public Policies to Private Business, University of Messina, Italy, 2018/6, pp. 276–284.

[25] H. Amini Toosi, M. Lavagna, Optimization and LCSA-based design method for energy retrofitting of existing buildings, in: Designing Sustainability for All, Proceedings of the 3rd LeNS World Distributed Conference, Milano, Mexico City, Beijing, Bangalore, Curitiba, Cape Town, vol. 1, 3-5 April 2019, ISBN 978-88-95651-26-2, pp. 1107–1111, 2019.

[26] S. Mahmoud, T. Zayed, M. Fahmy, Development of sustainability assessment tool for existing buildings, Sustain. Cities Soc. 44 (May 2017) 99–119, https://doi.org/10.1016/j.scs.2018.09.024, 2019.

[27] G. Akhanova, A. Nadeem, J.R. Kim, S. Azhar, A multi-criteria decision-making framework for building sustainability assessment in Kazakhstan, Sustain. Cities Soc. 52 (June 2019) 101842, https://doi.org/10.1016/j.scs.2019.101842, 2020.

[28] S. Amirhosain, A. Hammad, Developing surrogate ANN for selecting near-optimal building energy renovation methods considering energy consumption, LCC and LCA, J. Build. Eng. 25 (April) (2019) 100790, https://doi.org/10.1016/j.jobe.2019.100790.

[29] K. Amasyali, N.M. El-gohary, A review of data-driven building energy consumption prediction studies, Renew. Sustain. Energy Rev. 81 (September 2017) 1192–1205, https://doi.org/10.1016/j.rser.2017.04.095, 2018.

[30] P. Westermann, R. Evins, Surrogate modelling for sustainable building design – a review, Energy Build. 198 (Sep. 2019) 170–186, https://doi.org/10.1016/J.ENBUILD.2019.05.057.

[31] T. Hong, Z. Wang, X. Luo, W. Zhang, Energy & Buildings State-of-the-art on research and applications of machine learning in the building life cycle, Energy Build. 212 (2020) 109831, https://doi.org/10.1016/j.enbuild.2020.109831.

[32] C. Deb, F. Zhang, J. Yang, S. Eang, K. Wei, A review on time series forecasting techniques for building energy consumption, Renew. Sustain. Energy Rev. 74 (July 2016) 902–924, https://doi.org/10.1016/j.rser.2017.02.085, 2017.

[33] M. Bourdeau, E. Nefzaoui, X. Guo, P. Chatellier, Modeling and forecasting building energy consumption: a review of data- driven techniques, Sustain. Cities Soc. 48 (April) (2019) 101533, https://doi.org/10.1016/j.scs.2019.101533.

[34] F. P. Chantrelle, H. Lahmidi, W. Keilholz, M. El Mankibi, and P. Michel, "Development of a multicriteria tool for optimizing the renovation of buildings", Appl. Energy, vol. 88, no. 4, pp. 1386–1394, Apr. 2011, doi: 10.1016/J.APENERGY.2010.10.002.

[35] E. Antipova, D. Boer, G. Guillén-Gosálbez, L.F. Cabeza, L. Jiménez, Multi-objective optimization coupled with life cycle assessment for retrofitting buildings, Energy Build. 82 (Oct. 2014) 92–99, https://doi.org/10.1016/j.enbuild.2014.07.001.

[36] J. Carreras, D. Boer, G. Guillén-Gosálbez, L.F. Cabeza, M. Medrano, L. Jiménez, Multi-objective optimization of thermal modelled cubicles considering the total cost and life cycle environmental impact, Energy Build. 88 (Feb. 2015) 335–346, https://doi.org/10.1016/J.ENBUILD.2014.12.007.

[37] J. Carreras, et al., Systematic approach for the life cycle multi-objective optimization of buildings combining objective reduction and surrogate modeling, Energy Build. 130 (Oct. 2016) 506–518, https://doi.org/10.1016/j.enbuild.2016.07.062.

[38] S.K. Pal, A. Takano, K. Alanne, K. Siren, A life cycle approach to optimizing carbon footprint and costs of a residential building, Build. Environ. 123 (2017) 146–162, https://doi.org/10.1016/j.buildenv.2017.06.051.

[39] H. Ramin, P. Hanafizadeh, T. Ehterami, M.A. AkhavanBehabadi, Life cycle-based multi-objective optimization of wall structures in climate of Tehran, Adv. Build. Energy Res. 2549 (2017) 1–14, https://doi.org/10.1080/17512549.2017.1344137.

[40] P. Ylmén, K. Mjörnell, J. Berlin, J. Arfvidsson, The influence of secondary effects on global warming and cost optimization of insulation in the building envelope, Build. Environ. 118 (Jun. 2017) 174–183, https://doi.org/10.1016/J.BUILDENV.2017.03.019.

[41] G. Mauro, et al., A multi-step approach to assess the lifecycle economic impact of seismic risk on optimal energy retrofit, Sustainability 9 (6) (Jun. 2017) 989, https://doi.org/10.3390/su9060989.

[42] E. Mostavi, S. Asadi, D. Boussaa, Development of a new methodology to optimize building life cycle cost, environmental impacts, and occupant satisfaction, Energy 121 (Feb. 2017) 606–615, https://doi.org/10.1016/J.ENERGY.2017.01.049.

[43] J. Hester, J. Gregory, F.-J. Ulm, R. Kirchain, Building design-space exploration through quasi-optimization of life cycle impacts and costs, Build. Environ. 144 (Oct. 2018) 34–44, https://doi.org/10.1016/J.BUILDENV.2018.08.003.

[44] J. Jokisalo, P. Sankelo, J. Vinha, K. Sirén, R. Kosonen, Cost optimal energy performance renovation measures in a municipal service building in a cold climate, in: E3S Web of Conferences 111, CLIMA 2019 vol. 3022, 2019, https://doi.org/10.1051/e3sconf/201911103022, 201 9.

[45] S. Amirhosain, A. Hammad, Developing surrogate ANN for selecting near-optimal building energy renovation methods considering energy consumption, LCC and LCA, J. Build. Eng. 25 (April) (2019) 100790, https://doi.org/10.1016/j.jobe.2019.100790.

[46] J. Hirvonen, J. Jokisalo, J. Heljo, R. Kosonen, Optimization of emission reducing energy retrofits in Finnish apartment buildings, in: E3S Web of Conferences 111, CLIMA 2, 2019, https://doi.org/10.1051/e3sconf/2019111030, 2019, 2019.

[47] EN_15978, EN 15978:2011, Sustainability of Construction Works. Assessment of Environmental Performance of Buildings, Calculation method", 2011.

[48] S. Sala, E. Crenna, M. Secchi, R. Pant, Global Normalisation Factors for the Environmental Footprint and Life Cycle Assessment, 2017, p. 16, https://doi.org/10.2760/88930.

[49] V. Castellani, L. Benini, S. Sala, R. Pant, A distance-to-target weighting method for Europe 2020, Int. J. Life Cycle Assess. 21 (8) (2016) 1159–1169, https://doi.org/10.1007/s11367-016-1079-8.

[50] G. Huppes, L. Van Oers, Evaluation of Weighting Methods for Measuring the EU-27 Overall Environmental Impact, 2011, https://doi.org/10.2788/88465.

[51] EN_16627, EN 16627:2015 Sustainability of Construction Works. Assessment of Economic Performance of Buildings. Calculation Methods, 2015.

[52] ISO_15686-5, ISO 15686-5 Buildings and Constructed Assets. Service Life Planning. Life-Cycle Costing, 2017.

[53] EN 15643-3, EN 15643-3:2012 Sustainability of Construction Works - Assessment of Buildings - Part 3: Framework for the Assessment of Social Performance", 2012.

[54] EN_16309:2014+A1:2014, EN 16309:2014+A1:2014, Sustainability of Construction Works. Assessment of Social Performance of Buildings, Calculation methodology", 2014.

[55] I. Huertas-valdivia, A.M. Ferrari, D. Settembre-blundo, F.E. Garc, Social Life-Cycle Assessment: A Review by Bibliometric Analysis, 2020, pp. 1–25.

[56] A. Lehmann, E. Zschieschang, M. Traverso, Social Aspects for Sustainability Assessment of Technologies — Challenges for Social Life Cycle Assessment (SLCA), 2013, pp. 1581–1592, https://doi.org/10.1007/s11367-013-0594-0.

[57] R.J. Bonilla-alicea, K. Fu, Systematic Map of the Social Impact Assessment Field, 2019.

[58] O. Tokede, M. Traverso, Implementing the Guidelines for Social Life Cycle Assessment : Past, Present, and Future, 2020, pp. 1910–1929.

[59] M. Pizzol, A. Laurent, S. Sala, B. Weidema, F. Verones, C. Koffler, Normalisation and weighting in life cycle assessment: quo vadis? Int. J. Life Cycle Assess. 22 (6) (2017) 853–866, https://doi.org/10.1007/s11367-016-1199-1.

[60] S. Walker, W. Khan, K. Katic, W. Maassen, W. Zeiler, Energy & Buildings Accuracy of different machine learning algorithms and added-value of predicting aggregated-level energy performance of commercial buildings, Energy Build. 209 (2020) 109705, https://doi.org/10.1016/j.enbuild.2019.109705.

[61] A. Miglioli, C. Del Pero, F. Leonforte, N. Aste, Load matching in residential buildings through the use of thermal energy storages, in: International Conference on Clean Electrical Power (ICCEP), 2019, pp. 272–279.

[62] R. Andreas, S. Serenella, N. Jungbluth, Normalization and weighting: the open challenge in LCA, Int. J. Life Cycle Assess. (2020), https://doi.org/10.1007/s11367-020-01790-0.

[63] Ecoinvent 3.6, Ecoinvent 3.6, 2019 Database, 2019.

[64] Eurostat, 2019. https://ec.europa.eu/eurostat/data/database/.

[65] EU, EU statistics. https://www.euro-area-statistics.org/?lg=en, 2020.

[66] Statista, Business data platform. https://www.statista.com, 2020. (Accessed 5 August 2020).

[67] J. Salom, A.J. Marszal, J. Widen, J. Candanedo, K.B. Lindberg, Analysis of load match and grid interaction indicators in net zero energy buildings with simulated and monitored data, Appl. Energy 136 (2014) 119–131, https://doi.org/10.1016/j.apenergy.2014.09.018.

[68] B. Morvaj, R. Evins, J. Carmeliet, Decarbonizing the electricity grid: the impact on urban energy systems, distribution grids and district heating potential, Appl. Energy 191 (Apr. 2017) 125–140, https://doi.org/10.1016/J.APENERGY.2017.01.058.

[69] A. Marszal, N.R. Canada, K.B. Lindberg, Interaction Indicators in Net Zero Energy Buildings with High-Resolution Data, May 2015, 2014.